

Petrophysical Reservoir Characterisation and Flow Unit Assessment of D-3 Reservoir Sands Vin Field, Niger Delta

Onyewuchi Vin Chinedu¹ ; Minapuye, I.Odigi²

Department of Geology, University of Port Harcourt Port Harcourt Nigeria

Centre for Petroleum Geosciences, Institute of Petroleum Studies, University of Port Harcourt, Nigeria

Abstract:- Petrophysical evaluation and flow unit assessment of the D-3 reservoir sand in the Vin field, offshore Niger Delta has been performed. The aims of the study are to assess the reservoir quality and flow units in the field through the integration of results from core analysis, production data, seismic data, and petrophysical parameters. Well log suites from 22 wells comprising gamma ray, resistivity, neutron, density, seismic data, and ditch cutting samples were obtained and analyzed. Petrophysical evaluation was carried out using various petrophysical computations. Field wide correlation from the western to the eastern part of the field was also carried out. Assessment of the flow unit was done using Flow Zone Indicator (FZI), Stratified Modified Lorenz plot, porosity-permeability cross plot and Winland technique. Field wide correlation revealed that the reservoir is laterally extensive and thins towards the east. Reservoir rock qualities were generally very good with Volume of shale ranging from 0.08 to 0.14, with an average of 0.11. Porosity values ranges from 0.22 to 0.40 with an average value of 0.34 while permeability values is between 130mD to 10,000 mD, with an average value of 2692 mD. Average water saturation values ranges from 0.17 to 0.42, while the average net to gross ratio is 0.89. The bulk water volume values are nearly constant, meaning the reservoir is homogenous and at irreducible water saturation. This implies that the reservoir can produce water-free hydrocarbon. The Stratified Modified Lorenz (SML) plot revealed three flow units with two high speed zones (FZ 1 and FZ 3) and one low speed zone (FZ 2). Based on the FZI, three flow units (FZ-1 to FZ-3) were identified in the reservoir with FZ-1 having the best reservoir quality. Winland technique presents three Petrofacies (Mega porous, Macro porous, Micro porous). Porosity-permeability cross plot also revealed three distinct facies based on ditch cuttings description. These facies are: U1- fine grained well sorted sandstone, U2- very fine grained well sorted sandstone, and U3- very fine grained shaley sandstone. Each of these facies is associated to a unique flow unit meaning that different depositional environment and diagenetic processes control the geometry of the reservoir and consequently the flow unit index. By modelling the reservoir behaviour and simulating their behaviour, uncertainties associated with field development in the Vin field and fields in the eastern Niger Delta will be reduced from the outcome of this study.

Keywords:- Baffle, Heterogeneity, Flowzone, Syntedimentary, Dip Closure.

I. INTRODUCTION

Hydrocarbon reservoir characterization involves the quantification, integration, reduction and analysis of geological, petrophysical, seismic and production data (Tinker, 1996). It represents an indispensable tool for optimizing costly reservoir management decisions for hydrocarbon field development. The principal goal of reservoir characterization is to derive a spacial understanding of inter well heterogeneity and to produce a geological model. In reservoir evaluation and development, the assessment of petrophysical properties such as porosity, permeability, and water saturation, percentage of shale volume, mineralogy, and type of pore fluid are deduced from well logs, core analysis, and well tests. Core analysis is one of the reservoir assessment tools that directly measure many important formation properties. The analysis determines porosity, permeability, grain-size distribution, grain density, mineral composition, sensitivity of fluids, and effect of overburden stress (Bateman, 1985).

The Vin field is located (Fig 1) 30km offshore in the shallow waters of the eastern Niger Delta with an average water depth of 76ft. It was described as an elongate, four way dip close, rollover anticline containing two structural culminations which are separated by a saddle.

This study is focused on the petrophysical analysis, interpretation and the quantitative evaluation of reservoir properties in the wells. Special emphasis will be given to the most important parameters (porosity, water saturation and permeability, net to gross). The Stratified Modified Lorenz plot, Flow Zone Indicator plot, porosity-permeability plot and Winland plot were used to delineate the various flow units. Using the proposed integrated methodology has lead to a significantly more accurate petrophysical reservoir description and 3-D reservoir model, which can be used to forecast reservoir behavior and enhance recovery.

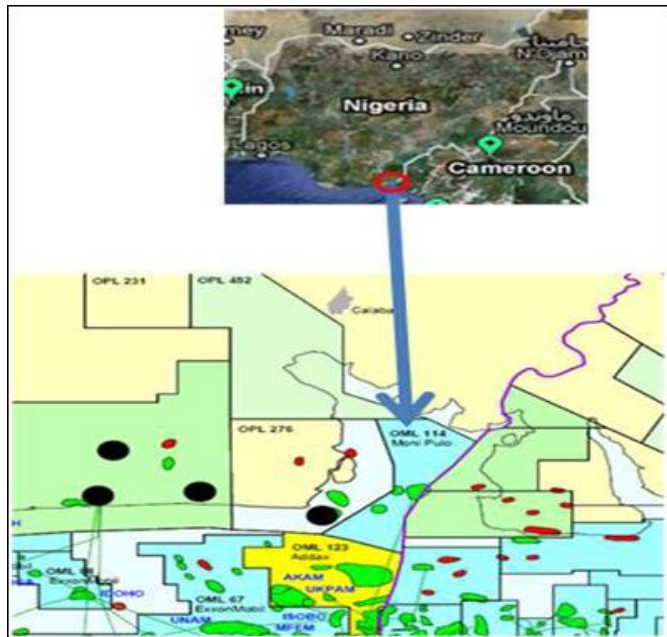


Fig 1 Location of Vin Field

II. GEOLOGY OF STUDY AREA

The geology of the Niger delta has been extensively discussed by several authors. The present study builds on work of Short & Stauble (1967), Weber (1971), Weber & Daukoru (1975), Evamy et al. (1978), Ejedawe (1981), Doust & Omatsola (1990), Reijers et al. (1996), (Reijers 2011). The evolution of the delta is controlled by pre- and syndimentary tectonics as described by Evamy et al. (1978), Knox & Omatsola (1987), Reijers et al., (1997) and Reijers (2011). The basin evolved following the separation of African and South American plates during the Early Cretaceous times. This was followed by the opening of the South Atlantic Ocean and several episodes of transgressions and regressions accounted for the sedimentary fills in both the Cretaceous and Tertiary.

The stratigraphy of the study area falls within the extensional Miocene to Pleistocene age (Fig. 2). The structural pattern is characterised by South dipping NE-SW trending growth faults and counter regional faults, which defined and controlled sedimentation especially the prospective Biafra Member and the Agbada Formation.

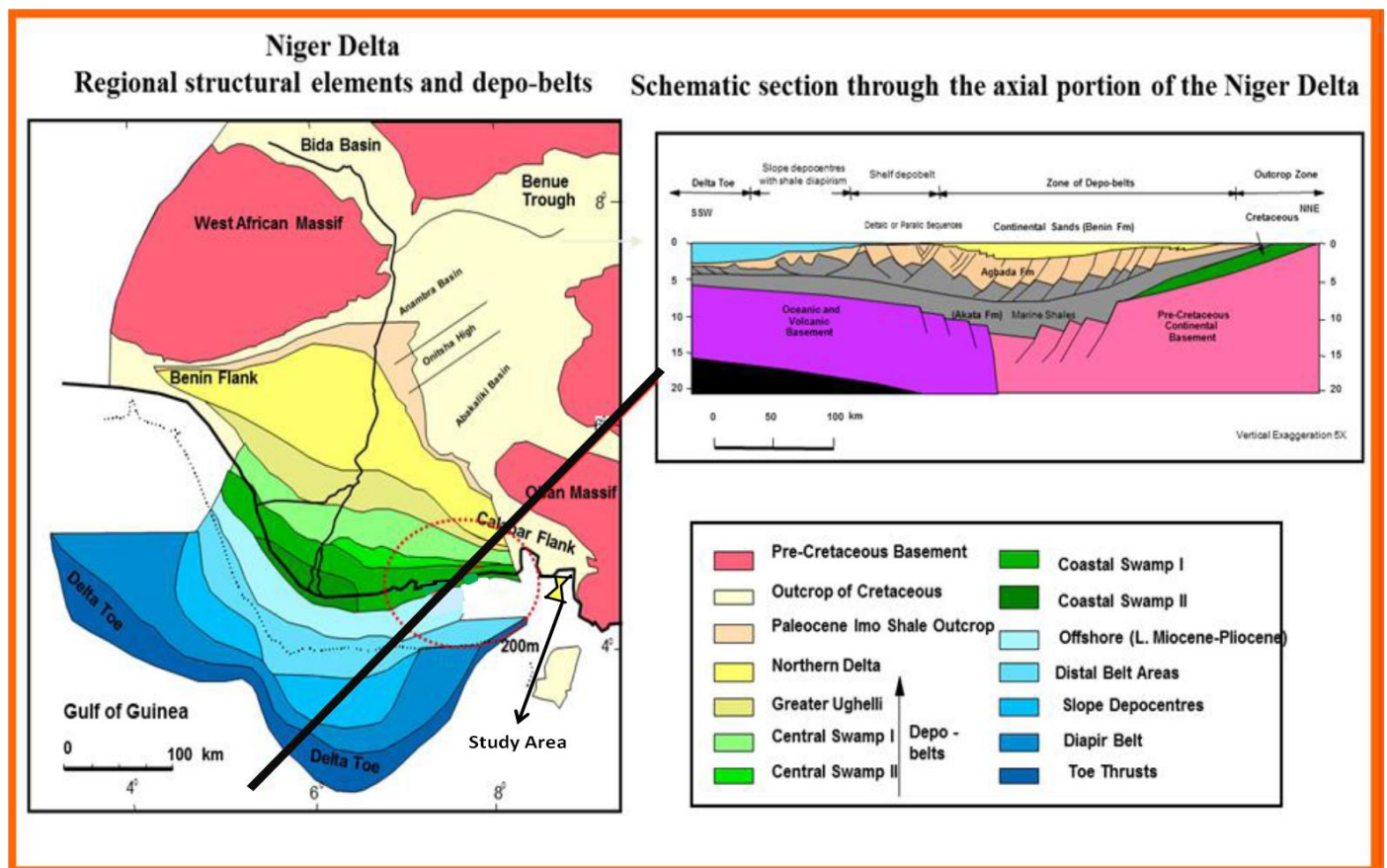


Fig 2 Regional Structural Element and Schematic Section through Eastern Niger Delta (Modified from Corredor et al., 2005)

The stratigraphic sequence in the southeastern flank of the Niger delta shows a marked facies change in comparison with the sequence in the central part of the delta. The Agbada formation in SE Niger delta is divided into four local members: D-1, Qua Iboe, Rubble and Biafra member (Figure 3) (Orife and Avbovbo., 1989).

From bottom to top, the eastern offshore stratigraphy (Fig. 3) is divided into:

AKATA SHALE of Middle Miocene age is Pro-deltaic and under-compacted dark shale deposited in deep marine environment.

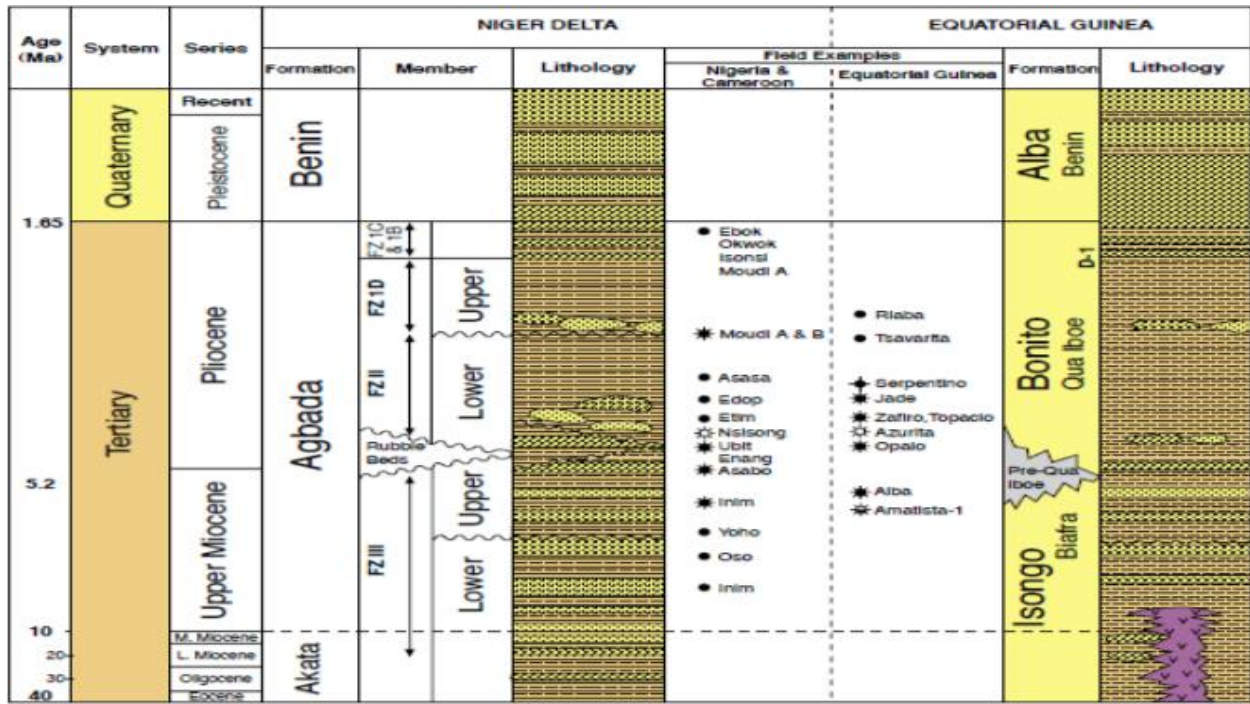


Fig 3 Lithostratigraphy of the Southeastern Niger Delta

AGBADA FORMATION, an alternating Upper Miocene to Pliocene ma-rine shales and fluvio-marine sands ranging from lower coastal plain to delta front environment which can be subdivided into:

- **BIAFRA Member**, a pro-grading old Miocene sandy deltaic system.
- **RUBBLE BEDS Member**, deposited during the transition Miocene- Pliocene.
- **KWA IBOE SHALE Member**, thick Pro-deltaic shales of early Plio-cene age.

- **D1 Member** which represents the upper sand bearing series of the prograding young Pliocene deltaic system.

SANDY BENIN FORMATION of Pleistocene to present age. The Benin Formation is the unconsolidated fresh water sand preceding Agbada Formation. Oil and gas accumulations have only been encountered in the Kwa Iboe, Rubble Beds, and mainly in the Biafra Member which contains the best reservoirs (Figure 4).

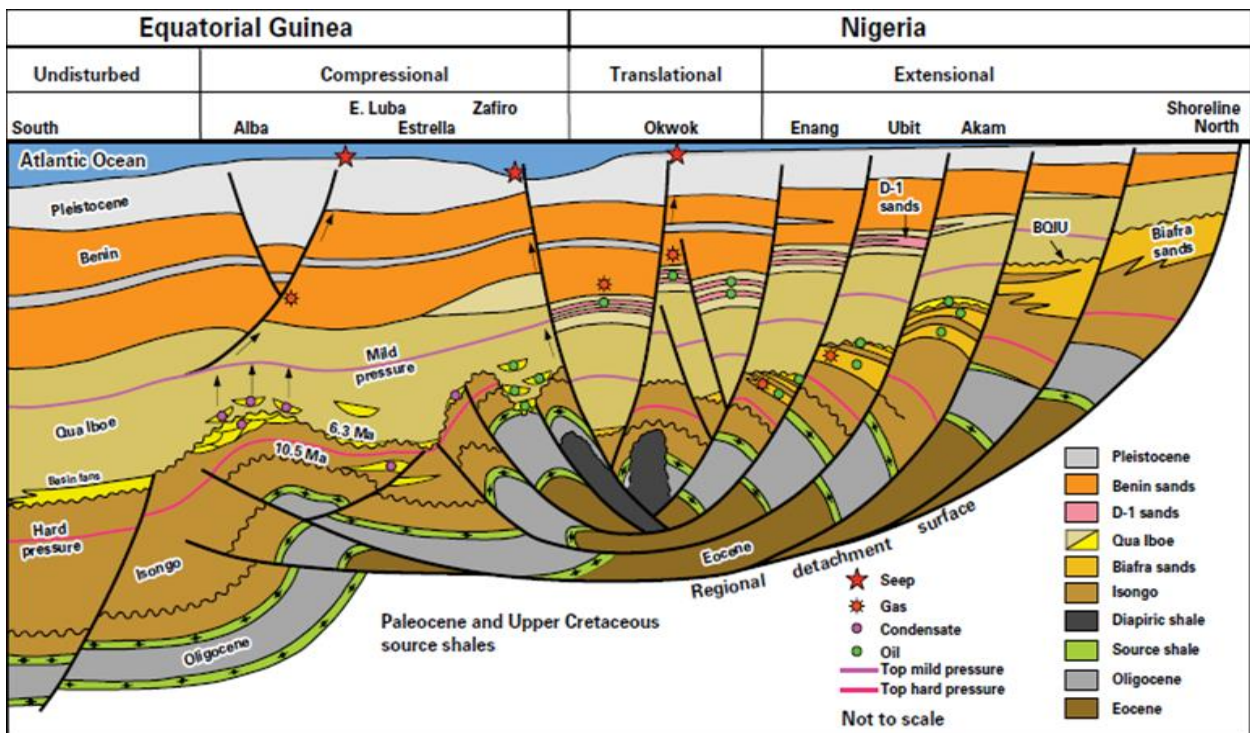


Fig 4 Stratigraphic Model of S-E Niger Delta (Joseph et al., 2004)

III. MATERIALS AND METHODS

The data used for this research was collected from Moni Pulo Limited under the auspices of Lulu Briggs chair, Institute of Petroleum Studies University of Port Harcourt. The data set include the following: Well data for 22 wells (exploratory, pilot, horizontal and injection wells), Surface location map of the wells, LWD logs (22 wells), Survey data (22 wells), 3D Seismic data, Core data for A2P2 (1 well) and wireline data.

The seismic dataset include 3D-Pre-stack data in SEG-Y format and well data (logs and picks) in various digital

The following petrophysical analysis were carried out for all the wells in the field from wireline logs by using petrophysical calculation (Archie, 1942; Asquith and Krygowski, 2004): Net-to-cross (N/G), Porosity , Permeability (K), Volume of Shale (Vsh), Formation factor, Water saturation (Sw), Irreducible water saturation (Swirr),

formats. The seismic and well data was loaded into Petrel database. Well log correlation and formation evaluation analysis were carried out with Gamma ray, resistivity, sonic, neutron and density logs. A combination of log suits (GR, neutron, density and resistivity), and petrophysical evaluation results (volume of shale, porosity and water saturation) were used in validating the top and base of the reservoir. The fluid contact and fluid in the reservoir were characterized using Neutron – density, bulk density and resistivity logs. The Gamma ray index was used to determine the percentage of shale and the dominant lithology.

Bulk Volume Water (BVW) and Hydrocarbon saturation (SH). Flow unit was identified using flow zone indicators (FZI) Amaefule et al., (1993), Modified Stratified Lorenze Plot, Winland plot and porosity-permeability cross-plot. Finally a model of the reservoirs sands in the Vin field was carried out based on the flowchart (Figure 5).

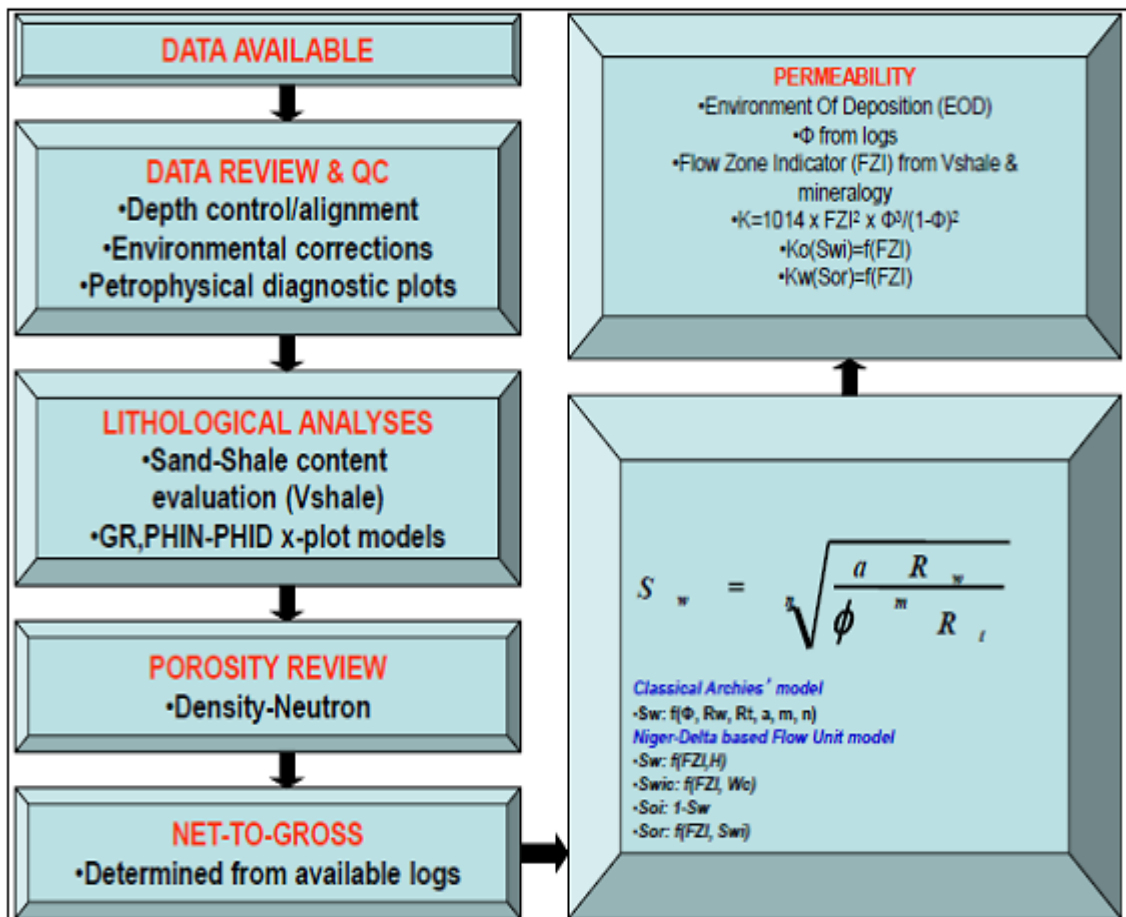


Fig 5 General Workflow for Petrophysical Analysis

IV. RESULTS AND DISCUSSION

➤ *Structure*

The study shows that the Vin field is characterized by rollover anticline associated with an E-W trending growth fault to the North (Figure 6A). It exhibits 4-way dip closure (Figure 6B) and two structural highs, Vin West and Vin East, separated by a saddle Figure 7. The structure is most

apparent within the Agbada formation, suggesting syndepositional development. The syndepositional growth faults activated at the delta front retards the advancement of the sandy Benin Formation. The down thrown part becomes the new focus of Agbada paralic facies deposition until subsidence stabilizes; by then a maximum thickness of Agbada Formation has been deposited (Ekweozor and Daukoru, 1984).

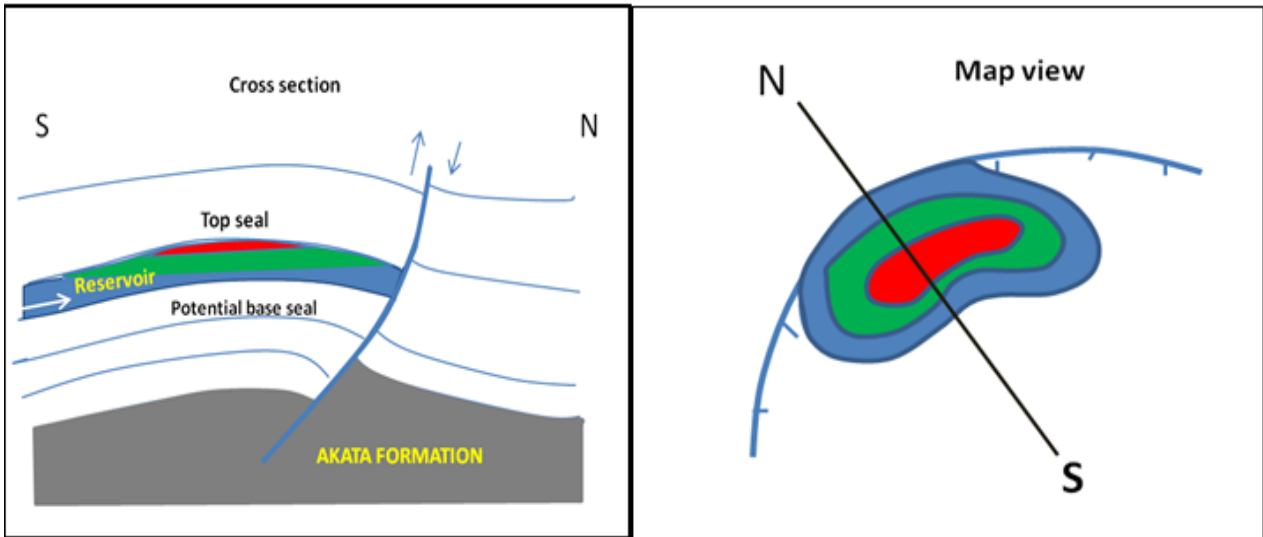


Fig 6 (A and B): Schematic Diagram Showing the Roll over Anticline and four way Dip Closure

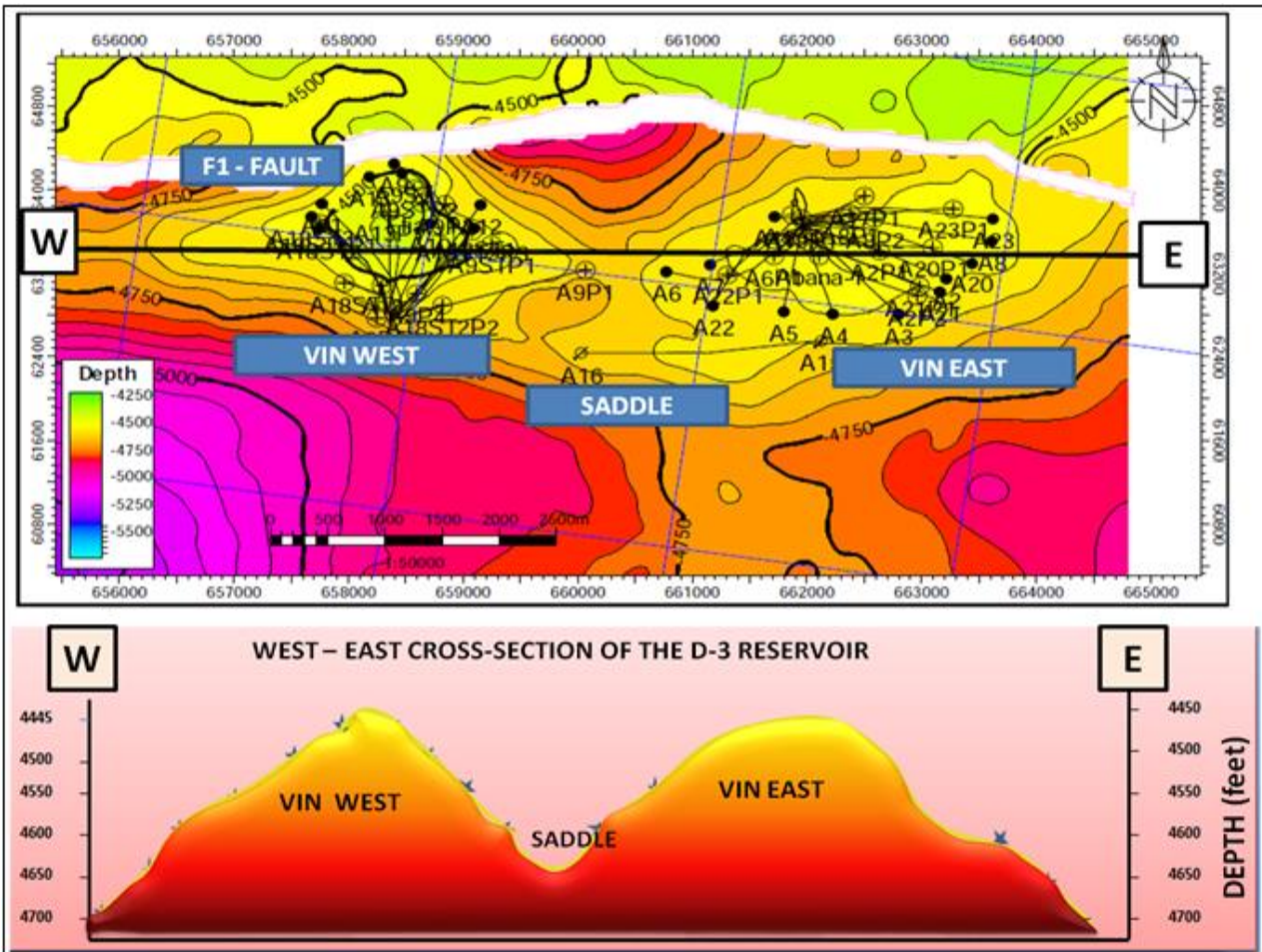


Fig 7 Stratigraphic Framework of D-5 Reservoir in Vin East

➤ *Stratigraphic Correlation*

Field wide correlation (Fig 8A and B) from the western to the eastern part of the field was also carried out. A transect passes through the selected wells. The transect line W – E connects wells (A9P2 – A16 – A15 – A2PA – A8). All depths for the stratigraphical correlations are true vertical depth subsea (SSTVD). An appropriate datum of 2000ft was chosen. This was the base of the Qua Iboe shale which is the first major regional shale marker typical of the

base of Benin sands. This marker shale is prominent on the Foot-wall and Hanging-wall of fault F1. It is a correlatable shale unit on well logs and is shown to cut across the entire well. The Qua Iboe Shale Member is considered to be part of the uppermost Agbada Formation (Whiteman, 1982). The D-3 reservoir has fairly constant thickness from one well to another, laterally extensive and cuts across all the wells in the field.

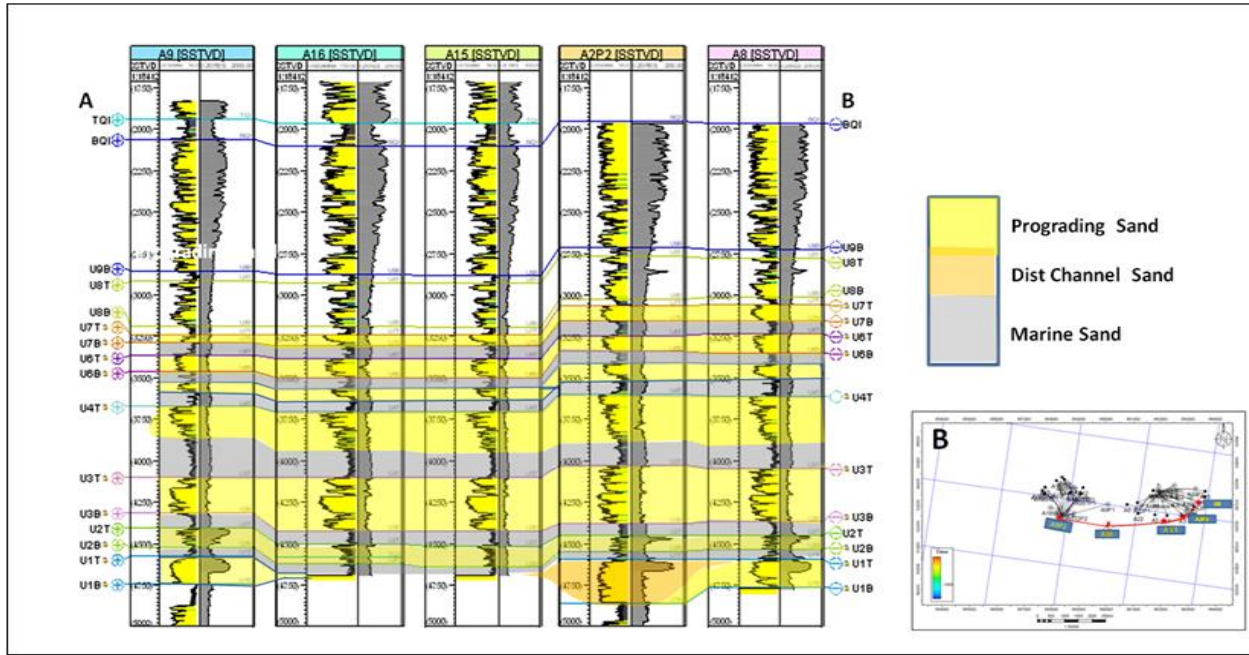


Fig 8 (A, B): A. Stratigraphic Correlation of Vin Field from West to East. B. The Transect Line W – E Connecting Wells (A9P2 – A16 – A15 – A2PA – A8)

➤ *Petrophysical Analysis*

Petrophysical evaluation of all the wells in the Vin field was carried out. This involves the use of empirical formulae to estimate the petrophysical properties of the D-3 reservoir. Open hole wireline log, core data and production history information was integrated in the analysis. The evaluated parameters were Volume of Shale, porosity (corrected for shale volume), Formation Factor, Water Saturation, Irreducible Water Saturation, Hydrocarbon Saturation, Bulk Volume Water and Permeability.

➤ *Petrophysical Summary*

The D-3 reservoir is of interest among all the reservoirs encountered in this study and it cuts across all the wells drilled in the field. Hydrocarbon potentials of the D-3 reservoir were revealed in their petrophysical properties. Petrophysical rock and fluid properties were evaluated for the reservoir (Table 1) and the Vin West has poor reservoir properties towards the top of D-3 reservoir while the reservoir properties for both Vin East and Vin West deteriorates towards the D-3 base.

Table 1 Average Reservoir Properties from the Petrophysical Analysis

	A2P2	A6P1	A8P1	A20P1	A23P1	A8P2	AVERAGE
GR _i	0.23	0.29	0.35	0.24	0.27	0.21	
V _{SH}	0.14	0.10	0.12	0.08	0.09	0.13	0.11
ϕ	0.34	0.33	0.34	0.28	0.31	0.32	0.32
F	7.78	6.79	6.33	7.12	5.29	6.92	
R _{w Cor}	0.24	0.15	0.21	0.14	0.31	0.20	
S _w	0.42	0.29	0.30	0.35	0.17	0.20	
S _{hc}	0.58	0.71	0.70	0.65	0.83	0.80	
BVW	0.08	0.26	0.23	0.27	0.05	0.22	
S _{wirr}	0.06	0.03	0.06	0.07	0.08	0.07	
K mD	3142.92	2339.8	3047.34	2236.0	3057.23	2333.45	2692
HCPV	0.23	0.25	0.24	0.18	0.05	0.19	
TOP DEPTH ft	-4545	-4547	-4540	-4520	-4542	-4537	
GOC ft	-4534	-4534	-4534	-4534	-4534	-4534	
OWC ft	-4601	-4601	-4601	-4610	-4601	-4601	
BOTTOM DEPTH ft	-4790	-4748	-4680	-4690	-4752	-4677	
GROSS THICKNESS ft	245	201	140	170	197	140	
NET PAY THICKNESS ft	56	76	61	90	68	64	
TOTAL V _{SH}	29.4	20.1	16.8	13.6	19.7	18.2	
NET THICKNESS ft	215.6	180.9	123.2	156.4	177.3	121.8	
N/G RATIO	0.88	0.90	0.88	0.92	0.89	0.87	
EFFECTIVE ϕ	0.30	0.29	0.30	0.30	0.297	0.29	

From this table, it can be derived that the Porosities of the reservoirs ranges from 0.28 – 0.34% with an average of 0.32%. Vertical and slight lateral variation was observed in the porosity in the field. This could be due to sedimentation process, diagenetic effect and the age of the sediment. Hydrocarbon saturation values ranging from 58% to 83%,

changes slightly from E-W and decreases down the depth with an average of 75%. Permeability value ranges from 130md to 10,000md, with an average value of 2692 md. Result from the reservoir properties shows that the reservoir quality is very good to excellent (Fig 9)

CLASSIFICATION OF SANDSTONE RESERVOIR			
Classification of sandstone reservoir based on porosity and permeability			
Percentage Porosity (%)	Qualitative Description	Average K_Value (md)	Qualitative Description
0 - 5	Negligible	<10.5	Poor to fair
5 - 10	Poor	15 – 50	Moderate
15 - 20	Good	50 – 250	Good
20 – 30	Very Good	250 – 1000	Very Good
> 30	Excellent	> 1000	Excellent
Etu-Efeotor, 1997			
Classification of sandstone reservoir based on shale contents			
Clean sand	<5% Vshale		
Slightly shaly sand	5 – 15 % Vshale		
Shaly sand	15 – 25% Vshale		
Very shaly sand	25 – 35% Vshale		
Shales	>35% Vshale		
David K Davies , 2002			

Fig 9 Reservoir quality of the D-5 reservoir sand (Modified from Etu- Efeotor 1997 and Davies 2002)

➤ *Bulk Volume Water*

The product of the formation water saturation (Sw) and its porosity (ϕ) is the bulk volume of water (BVW). Table 2, shows the variation of the BVW with depth for the A2P2 core sample. According to (Asquith and Gibson, 2001), if the value of the BVW calculated at various depth in a formation are constant or close to constant, this indicates that it is homogeneous and at irreducible water saturation. A

formation not at irreducible water saturation will exhibit wide variation in bulk volume water values.

From the study, it was shown that the values of the BVW with depth is almost constant, indicating that the reservoir is fairly homogeneous (Fig 10) and at irreducible water saturation. Hydrocarbon production from a zone of irreducible water saturation should be water free.

Table 2 Spread Sheet Showing Calculation for BVW for Core A2P2

Depth	PHIT	SW	BWV
5054	0.3878788	0.1124661	0.0436232
5054.5	0.3878788	0.1168462	0.0453222
5055	0.3878788	0.1142306	0.0443076
5055.5	0.3878788	0.1124661	0.0436232
5056	0.3878788	0.1094634	0.0424585
5056.5	0.3878788	0.1006224	0.0390293
5057	0.3939394	0.104487	0.0411615
5057.5	0.3939394	0.1020071	0.0401846
5058	0.3818182	0.09495048	0.0362538
5058.5	0.3818182	0.1051294	0.0401403
5059	0.3818182	0.09424233	0.0359834
5059.5	0.3878788	0.09964222	0.0386491
5060	0.3878788	0.09662266	0.0374779

5060.5	0.3939394	0.0903929	0.0356093
5061	0.3939394	0.09484798	0.0373644
5061.5	0.3818182	0.09601846	0.0366616
5062	0.3757576	0.09497608	0.035688
5062.5	0.3757576	0.0931254	0.0349926
5063	0.3757576	0.09423201	0.0354084
5063.5	0.3818182	0.09278864	0.0354284
5064	0.3878788	0.09138961	0.0354481
5064.5	0.3878788	0.09491413	0.0368152
5065	0.3878788	0.09595006	0.037217
5065.5	0.3818182	0.09705991	0.0370592
5066	0.3878788	0.09697138	0.0376131
5066.5	0.4	0.09543062	0.0381722
5067	0.4	0.1023613	0.0409445

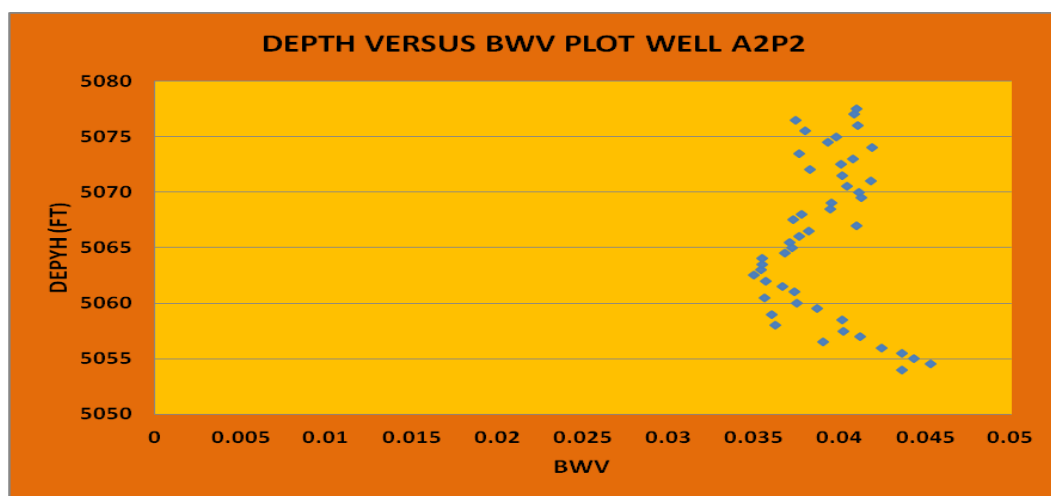


Fig 10 Plot of Depth (Ft) Versus Bulk Water Volume

➤ *Flow Unit Characterisation*

A flow unit is defined as a mappable portion of the total reservoir, within which geological and petrophysical properties that affect the flow of fluids are consistent and predictably different from the properties of other reservoir rock volume (Ebanks et al., 1992). There are various methods for defining and describing flow unit. In this study, the Stratified Modified Lorenz plot, Flow Zone Indicator plot and Winland plot were used to delineate flow units.

➤ *Stratified Modified Lorenz Plot (SML)*

The SML plot is a crossplot of “cumulative flow capacity “ - defined as a product of average permeability and thickness of an interval(Kh) –versus cumulative storage capacity – define as a product of average porosity and thickness of the same interval (ϕh). (Slatt, 2006), explained that this method was used because it requires only routine porosity and permeability data from logs and cores and is independent on facies identification, and uses simple cross plotting technique .

Table 3 Showing the Cumulative Flow Capacity and Cumulative Storage Capacity Distribution for the A2P2 Core Sample, D-3 Reservoir

H	K	ϕ	Kh	Σkh	$\Sigma kh/Sumkh$	ϕh	$\Sigma \phi h$	$\Sigma \phi h/Sum\phi h$	CFC	CSC
(m)	(md)	(fraction)	(md-m)	(md-m)		(m)	(m)			
0.21	1.60	24.5	0.3	0.3	0.000	5.2	5.2	0.002	0.000	0.002
0.55	0.7	23.1	0.4	0.7	0.000	12.7	17.9	0.006	0.000	0.006
0.59	46.	25.8	27.3	28.1	0.000	15.3	33.3	0.010	0.000	0.010
0.53	99.	27.0	52.8	80.9	0.000	14.4	47.7	0.015	0.000	0.015
0.50	319.	29.9	160.4	241.3	0.001	15.0	62.7	0.020	0.001	0.020
0.20	295.	30.6	58.4	299.7	0.001	6.1	68.8	0.022	0.001	0.022
0.82	331.	30.5	272.4	572.1	0.002	25.1	93.9	0.029	0.002	0.029
0.24	281.	30.8	68.5	640.6	0.002	7.5	101.4	0.032	0.002	0.032
0.53	511.	32.7	272.6	913.2	0.003	17.5	118.9	0.037	0.003	0.037
0.30	517.	32.8	157.6	1070.8	0.003	10.0	128.9	0.040	0.003	0.040

0.49	365.	32.4	178.0	1248.8	0.003	15.8	144.7	0.045	0.003	0.045
0.30	1080.	34.6	329.2	1577.9	0.004	10.6	155.2	0.049	0.004	0.049
0.24	1730.	33.0	421.8	1999.8	0.006	8.0	163.3	0.051	0.006	0.051
0.17	59.	30.1	9.9	2009.6	0.006	5.0	168.3	0.053	0.006	0.053
0.34	140.	29.1	46.9	2056.6	0.006	9.8	178.1	0.056	0.006	0.056
0.32	19.	30.1	6.1	2062.7	0.006	9.6	187.7	0.059	0.006	0.059
0.26	174.	30.0	45.1	2107.7	0.006	7.8	195.5	0.061	0.006	0.061
0.06	142.	30.5	8.7	2116.4	0.006	1.9	197.3	0.062	0.006	0.062
0.21	82.	30.4	17.5	2133.9	0.006	6.5	203.8	0.064	0.006	0.064
0.49	300.	31.7	146.3	2280.2	0.006	15.4	219.2	0.069	0.006	0.069
0.26	129.	30.2	33.4	2313.6	0.006	7.8	227.1	0.071	0.006	0.071
0.14	323.	32.1	44.3	2357.9	0.006	4.4	231.5	0.072	0.006	0.072
0.17	44.	28.3	7.4	2365.3	0.007	4.7	236.2	0.074	0.007	0.074
0.23	4.1	25.2	0.9	2366.2	0.007	5.8	242.0	0.076	0.007	0.076
0.15	8.9	26.5	1.4	2367.6	0.007	4.0	246.0	0.077	0.007	0.077
0.24	4.1	24.7	1.0	2368.6	0.007	6.0	252.0	0.079	0.007	0.079
0.24	1.3	22.9	0.3	2368.9	0.007	5.6	257.6	0.081	0.007	0.081
0.46	5.9	26.5	2.7	2371.6	0.007	12.1	269.7	0.084	0.007	0.084
0.58	0.33	19.2	0.2	2371.8	0.007	11.1	280.8	0.088	0.007	0.088
0.24	37.	26.6	9.0	2380.8	0.007	6.5	287.3	0.090	0.007	0.090
0.43	47.	26.3	20.1	2400.9	0.007	11.2	298.6	0.093	0.007	0.093
0.24	306.	31.5	74.6	2475.5	0.007	7.7	306.2	0.096	0.007	0.096
0.43	94.	26.9	40.1	2515.6	0.007	11.5	317.7	0.099	0.007	0.099
0.27	3680.	33.8	1009.4	3525.0	0.010	9.3	327.0	0.102	0.010	0.102
0.32	5240.	36.1	1676.9	5202.0	0.014	11.5	338.5	0.106	0.014	0.106
0.38	3860.	36.6	1470.6	6672.5	0.018	14.0	352.5	0.110	0.018	0.110
0.37	1890.	35.2	691.3	7363.8	0.020	12.9	365.3	0.114	0.020	0.114
0.23	1800.	32.2	411.5	7775.3	0.021	7.4	372.7	0.117	0.021	0.117
0.41	1680.	34.7	691.3	8466.5	0.023	14.3	387.0	0.121	0.023	0.121
0.27	4240.	35.4	1163.1	9629.6	0.026	9.7	396.7	0.124	0.026	0.124
0.35	3310.	33.0	1160.2	10789.7	0.030	11.6	408.2	0.128	0.030	0.128
0.62	3300.	33.2	2061.9	12851.6	0.035	20.8	429.0	0.134	0.035	0.134
0.30	2930.	33.5	893.0	13744.6	0.038	10.2	439.2	0.138	0.038	0.138
0.27	1900.	33.5	521.2	14265.8	0.039	9.2	448.4	0.140	0.039	0.140
0.46	2111.	33.4	965.1	15230.9	0.042	15.3	463.7	0.145	0.042	0.145
0.37	2180.	34.6	797.3	16028.2	0.044	12.6	476.3	0.149	0.044	0.149
0.24	2420.	34.8	590.1	16618.3	0.046	8.5	484.8	0.152	0.046	0.152
0.24	3280.	35.4	799.8	17418.0	0.048	8.6	493.4	0.155	0.048	0.155
0.15	5300.	36.8	807.7	18225.7	0.050	5.6	499.0	0.156	0.050	0.156
0.29	4480.	34.9	1297.2	19522.9	0.054	10.1	509.1	0.159	0.054	0.159
0.21	6600.	35.9	1408.1	20931.0	0.058	7.6	516.8	0.162	0.058	0.162
0.55	5690.	36.3	3121.6	24052.6	0.066	19.9	536.7	0.168	0.066	0.168
0.47	7660.	34.8	3618.7	27671.3	0.076	16.5	553.2	0.173	0.076	0.173
0.53	7050.	34.6	3760.3	31431.6	0.086	18.5	571.7	0.179	0.086	0.179
0.21	4470.	35.1	953.7	32385.3	0.089	7.5	579.1	0.181	0.089	0.181
0.24	4480.	34.9	1092.3	33477.6	0.092	8.5	587.6	0.184	0.092	0.184
0.09	4580.	35.5	418.8	33896.4	0.093	3.2	590.9	0.185	0.093	0.185
0.27	5630.	36.3	1544.3	35440.8	0.098	10.0	600.8	0.188	0.098	0.188
0.41	1380.	35.7	567.8	36008.6	0.099	14.7	615.5	0.193	0.099	0.193
0.41	3000.	35.6	1234.4	37242.9	0.102	14.6	630.2	0.197	0.102	0.197
0.47	4080.	36.5	1927.5	39170.4	0.108	17.3	647.4	0.203	0.108	0.203
0.35	3500.	35.0	1226.8	40397.2	0.111	12.3	659.7	0.207	0.111	0.207
0.30	1480.	35.7	451.1	40848.2	0.112	10.9	670.6	0.210	0.112	0.210
0.21	5470.	37.3	1167.0	42015.3	0.116	8.0	678.5	0.213	0.116	0.213
0.55	4620.	35.7	2534.6	44549.9	0.123	19.6	698.1	0.219	0.123	0.219
0.24	5530.	36.1	1348.4	45898.2	0.126	8.8	706.9	0.221	0.126	0.221
0.24	3620.	35.9	882.7	46780.9	0.129	8.8	715.7	0.224	0.129	0.224
0.46	3210.	35.7	1467.5	48248.4	0.133	16.3	732.0	0.229	0.133	0.229
0.52	3900.	36.4	2020.7	50269.2	0.138	18.9	750.9	0.235	0.138	0.235

0.20	4620.	35.6	915.3	51184.4	0.141	7.0	757.9	0.237	0.141	0.237
0.20	3612.	34.5	715.6	51900.0	0.143	6.8	764.7	0.240	0.143	0.240
0.27	3220.	35.5	883.3	52783.3	0.145	9.7	774.5	0.243	0.145	0.243
0.34	3720.	35.7	1247.2	54030.4	0.149	12.0	786.5	0.246	0.149	0.246
0.27	3130.	34.6	858.6	54889.0	0.151	9.5	796.0	0.249	0.151	0.249
0.24	3980.	35.5	970.4	55859.5	0.154	8.7	804.6	0.252	0.154	0.252
0.17	3810.	35.3	638.7	56498.1	0.155	5.9	810.5	0.254	0.155	0.254
0.24	3490.	35.7	851.0	57349.1	0.158	8.7	819.2	0.257	0.158	0.257
0.37	3427.	33.9	1253.4	58602.5	0.161	12.4	831.6	0.260	0.161	0.260
0.64	4280.	33.9	2739.4	61341.9	0.169	21.7	853.4	0.267	0.169	0.267
1.04	2360.	35.1	2445.6	63787.5	0.176	36.4	889.7	0.279	0.176	0.279
0.61	5590.	35.5	3407.5	67195.0	0.185	21.7	911.4	0.285	0.185	0.285
0.26	4250.	35.9	1101.0	68296.0	0.188	9.3	920.7	0.288	0.188	0.288
0.94	5620.	35.6	5310.0	73606.0	0.203	33.7	954.4	0.299	0.203	0.299
0.50	4910.	34.3	2469.2	76075.2	0.209	17.2	971.6	0.304	0.209	0.304
0.35	5950.	35.5	2085.5	78160.7	0.215	12.4	984.0	0.308	0.215	0.308
0.49	5780.	33.8	2818.7	80979.4	0.223	16.5	1000.5	0.313	0.223	0.313
0.47	5240.	34.7	2475.5	83454.8	0.230	16.4	1017.0	0.318	0.230	0.318
0.27	6070.	35.2	1665.0	85119.9	0.234	9.7	1026.6	0.322	0.234	0.322
0.24	4020.	34.9	980.2	86100.1	0.237	8.5	1035.1	0.324	0.237	0.324
0.43	1190.	34.1	507.8	86607.8	0.238	14.6	1049.7	0.329	0.238	0.329
0.27	6480.	35.8	1777.5	88385.3	0.243	9.8	1059.5	0.332	0.243	0.332
0.27	6430.	36.1	1763.8	90149.1	0.248	9.9	1069.4	0.335	0.248	0.335
0.21	942.	36.0	201.0	90350.1	0.249	7.7	1077.1	0.337	0.249	0.337
0.27	5130.	35.9	1407.2	91757.3	0.252	9.8	1087.0	0.340	0.252	0.340
0.24	5070.	35.8	1236.2	92993.5	0.256	8.7	1095.7	0.343	0.256	0.343
0.11	6070.	36.8	647.5	93641.0	0.258	3.9	1099.6	0.344	0.258	0.344
0.61	5250.	33.3	3200.2	96841.3	0.266	20.3	1119.9	0.351	0.266	0.351
0.49	5060.	35.2	2467.5	99308.8	0.273	17.1	1137.1	0.356	0.273	0.356
0.20	3580.	35.1	709.2	100018.0	0.275	6.9	1144.0	0.358	0.275	0.358
0.50	1040.	34.3	523.0	100541.1	0.277	17.2	1161.3	0.364	0.277	0.364
0.37	1500.	34.1	548.6	101089.7	0.278	12.5	1173.7	0.368	0.278	0.368
0.55	2660.	34.1	1459.3	102549.0	0.282	18.7	1192.4	0.373	0.282	0.373
0.46	4220.	34.6	1929.3	104478.3	0.287	15.8	1208.3	0.378	0.288	0.378
0.43	2740.	36.1	1169.2	105647.4	0.291	15.4	1223.7	0.383	0.291	0.383
0.23	2930.	36.4	669.8	106317.2	0.293	8.3	1232.0	0.386	0.293	0.386
0.21	3260.	35.7	695.5	107012.7	0.294	7.6	1239.6	0.388	0.294	0.388
0.40	4170.	35.0	1652.2	108665.0	0.299	13.9	1253.5	0.393	0.299	0.393
0.30	4570.	35.2	1392.9	110057.8	0.303	10.7	1264.2	0.396	0.303	0.396
0.37	2900.	35.1	1060.7	111118.5	0.306	12.8	1277.0	0.400	0.306	0.400
0.24	3930.	34.3	958.2	112076.7	0.308	8.4	1285.4	0.403	0.308	0.403
0.27	3290.	34.7	902.5	112979.2	0.311	9.5	1294.9	0.406	0.311	0.406
0.20	3740.	35.1	740.9	113720.1	0.313	7.0	1301.9	0.408	0.313	0.408
0.34	4800.	35.5	1609.3	115329.4	0.317	11.9	1313.8	0.411	0.317	0.411
0.49	2210.	33.9	1077.7	116407.1	0.320	16.5	1330.3	0.417	0.320	0.417
0.18	1200.	33.8	219.4	116626.5	0.321	6.2	1336.5	0.419	0.321	0.419
0.58	1620.	33.5	938.1	117564.7	0.323	19.4	1355.9	0.425	0.324	0.425
0.44	1800.	32.9	795.5	118360.2	0.326	14.5	1370.5	0.429	0.326	0.429
0.37	1520.	34.0	555.9	118916.1	0.327	12.4	1382.9	0.433	0.327	0.433
0.32	3228.	34.6	1033.0	119949.1	0.330	11.1	1394.0	0.437	0.330	0.437
0.43	3320.	32.5	1416.6	121365.8	0.334	13.9	1407.8	0.441	0.334	0.441
0.47	3320.	34.1	1568.4	122934.2	0.338	16.1	1424.0	0.446	0.338	0.446
0.17	4230.	33.8	709.1	123643.3	0.340	5.7	1429.6	0.448	0.340	0.448
0.05	5630.	33.5	257.4	123900.7	0.341	1.5	1431.2	0.448	0.341	0.448
0.09	7750.	35.4	708.6	124609.3	0.343	3.2	1434.4	0.449	0.343	0.449
0.66	6460.	33.5	4233.2	128842.5	0.355	21.9	1456.3	0.456	0.355	0.456
0.38	3220.	28.7	1226.8	130069.2	0.358	10.9	1467.3	0.460	0.358	0.460
0.23	3450.	29.8	788.6	130857.8	0.360	6.8	1474.1	0.462	0.360	0.462
0.46	6370.	32.9	2912.2	133770.1	0.368	15.0	1489.1	0.466	0.368	0.466

0.34	4280.	31.7	1434.9	135205.0	0.372	10.6	1499.7	0.470	0.372	0.470
0.26	5960.	33.6	1544.0	136749.0	0.376	8.7	1508.4	0.472	0.376	0.472
0.43	4000.	32.2	1706.8	138455.8	0.381	13.7	1522.2	0.477	0.381	0.477
0.24	2800.	34.1	682.7	139138.6	0.383	8.3	1530.5	0.479	0.383	0.479
0.06	2830.	34.3	172.5	139311.1	0.383	2.1	1532.6	0.480	0.383	0.480
0.15	4530.	34.3	690.3	140001.4	0.385	5.2	1537.8	0.482	0.385	0.482
0.40	4080.	33.5	1616.6	141618.0	0.390	13.3	1551.1	0.486	0.390	0.486
0.87	4350.	32.4	3778.6	145396.6	0.400	28.1	1579.2	0.495	0.400	0.495
0.17	5420.	32.6	908.6	146305.1	0.403	5.5	1584.6	0.496	0.403	0.496
0.24	5080.	32.1	1238.6	147543.8	0.406	7.8	1592.5	0.499	0.406	0.499
1.28	3900.	32.3	4992.4	152536.1	0.420	41.4	1633.8	0.512	0.420	0.512
0.52	5040.	33.5	2611.4	155147.5	0.427	17.4	1651.2	0.517	0.427	0.517
0.24	1440.	31.6	351.1	155498.7	0.428	7.7	1658.9	0.520	0.428	0.520
0.11	2660.	32.5	283.8	155782.4	0.429	3.5	1662.4	0.521	0.429	0.521
0.23	5360.	35.2	1225.2	157007.7	0.432	8.1	1670.4	0.523	0.432	0.523
0.08	5970.	34.2	454.9	157462.5	0.433	2.6	1673.0	0.524	0.433	0.524
0.52	4510.	33.7	2336.8	159799.3	0.440	17.4	1690.5	0.529	0.440	0.529
0.37	4690.	33.6	1715.3	161514.7	0.444	12.3	1702.7	0.533	0.444	0.533
0.09	1170.	31.9	107.0	161621.6	0.445	2.9	1705.7	0.534	0.445	0.534
0.49	2950.	34.2	1438.6	163060.2	0.449	16.7	1722.4	0.539	0.449	0.539
0.21	6760.	31.4	1442.2	164502.5	0.453	6.7	1729.1	0.542	0.453	0.542
0.27	6350.	32.4	1741.8	166244.3	0.457	8.9	1737.9	0.544	0.457	0.544
0.91	3490.	31.1	3191.1	169435.4	0.466	28.5	1766.4	0.553	0.466	0.553
0.38	4340.	31.0	1653.5	171088.9	0.471	11.8	1778.2	0.557	0.471	0.557
0.34	3800.	30.5	1274.0	172362.9	0.474	10.2	1788.4	0.560	0.474	0.560
0.38	3250.	32.4	1238.2	173601.1	0.478	12.4	1800.8	0.564	0.478	0.564
0.24	3060.	34.7	746.1	174347.2	0.480	8.4	1809.2	0.567	0.480	0.567
0.30	2340.	34.3	713.2	175060.4	0.482	10.5	1819.7	0.570	0.482	0.570
0.29	3820.	33.6	1106.1	176166.4	0.485	9.7	1829.4	0.573	0.485	0.573
0.02	5330.	34.9	81.2	176247.7	0.485	0.5	1829.9	0.573	0.485	0.573
0.30	1900.	25.9	579.1	176826.8	0.487	7.9	1837.8	0.576	0.487	0.576
0.55	399.	22.6	218.9	177045.7	0.487	12.4	1850.2	0.579	0.487	0.579
0.52	6900.	34.5	3575.1	180620.8	0.497	17.9	1868.1	0.585	0.497	0.585
0.84	6400.	34.8	5364.2	185985.0	0.512	29.1	1897.3	0.594	0.512	0.594
0.38	3510.	34.0	1337.2	187322.2	0.515	12.9	1910.2	0.598	0.515	0.598
0.34	3590.	33.0	1203.6	188525.8	0.519	11.1	1921.3	0.602	0.519	0.602
0.24	2230.	33.6	543.7	189069.6	0.520	8.2	1929.5	0.604	0.520	0.604
0.52	2260.	33.4	1171.0	190240.6	0.523	17.3	1946.8	0.610	0.524	0.610
0.17	1960.	27.8	328.6	190569.1	0.524	4.7	1951.4	0.611	0.524	0.611
0.35	2250.	25.6	788.6	191357.8	0.527	9.0	1960.4	0.614	0.527	0.614
0.26	2300.0	24.2	595.9	191953.6	0.528	6.3	1966.7	0.616	0.528	0.616
0.26	1520.	27.9	393.8	192347.4	0.529	7.2	1973.9	0.618	0.529	0.618
0.62	630.	27.9	393.6	192741.0	0.530	17.4	1991.3	0.624	0.530	0.624
0.38	4250.	35.2	1619.2	194360.2	0.535	13.4	2004.8	0.628	0.535	0.628
0.20	5480.	35.2	1085.6	195445.8	0.538	7.0	2011.7	0.630	0.538	0.630
0.41	7800.	36.3	3209.4	198655.2	0.547	14.9	2026.7	0.635	0.547	0.635
0.26	10260.	33.3	2658.0	201313.3	0.554	8.6	2035.3	0.637	0.554	0.637
0.53	1710.	34.3	912.1	202225.3	0.556	18.3	2053.6	0.643	0.556	0.643
0.27	3500.	33.2	960.1	203185.4	0.559	9.1	2062.7	0.646	0.559	0.646
0.14	1290.	33.6	176.9	203362.3	0.560	4.6	2067.3	0.647	0.560	0.647
0.34	4300.	35.2	1441.6	204804.0	0.564	11.8	2079.1	0.651	0.564	0.651
0.43	1490.	32.1	635.8	205439.7	0.565	13.7	2092.8	0.655	0.565	0.655
0.23	4300.	32.6	982.9	206422.7	0.568	7.5	2100.2	0.658	0.568	0.658
0.26	7180.	32.8	1860.1	208282.8	0.573	8.5	2108.8	0.660	0.573	0.660
0.20	4670.	32.1	925.2	209208.0	0.576	6.4	2115.1	0.662	0.576	0.662
0.24	5150.	34.0	1255.7	210463.7	0.579	8.3	2123.4	0.665	0.579	0.665
0.09	4720.	32.0	431.6	210895.2	0.580	2.9	2126.3	0.666	0.580	0.666
0.46	5220.	31.3	2386.5	213281.7	0.587	14.3	2140.6	0.670	0.587	0.670
0.29	4700.	31.1	1360.9	214642.6	0.591	9.0	2149.7	0.673	0.591	0.673

0.52	2010.	30.1	1041.5	215684.0	0.593	15.6	2165.3	0.678	0.594	0.678
0.15	4340.	30.6	661.4	216345.4	0.595	4.7	2169.9	0.680	0.595	0.680
0.27	5410.	31.9	1484.0	217829.4	0.599	8.8	2178.7	0.682	0.599	0.682
0.18	7680.	32.7	1404.4	219233.9	0.603	6.0	2184.7	0.684	0.603	0.684
0.24	3540.	33.9	863.2	220097.0	0.606	8.3	2192.9	0.687	0.606	0.687
0.09	3020.	33.5	276.1	220373.1	0.606	3.1	2196.0	0.688	0.606	0.688
0.34	3030.	34.6	1015.8	221389.0	0.609	11.6	2207.6	0.691	0.609	0.691
0.24	2900.	34.8	707.1	222096.1	0.611	8.5	2216.1	0.694	0.611	0.694
0.08	6530.	35.2	497.6	222593.7	0.612	2.7	2218.8	0.695	0.613	0.695
0.82	3020.	34.2	2485.2	225078.9	0.619	28.1	2246.9	0.704	0.619	0.704
0.30	4410.	34.0	1344.1	226423.0	0.623	10.4	2257.3	0.707	0.623	0.707
1.05	4520.	34.2	4752.8	231175.8	0.636	36.0	2293.3	0.718	0.636	0.718
0.26	4100.	35.1	1062.2	232238.0	0.639	9.1	2302.4	0.721	0.639	0.721
0.40	6280.	33.5	2488.3	234726.2	0.646	13.3	2315.6	0.725	0.646	0.725
0.15	3000.	32.9	457.2	235183.4	0.647	5.0	2320.6	0.727	0.647	0.727
0.15	4190.	32.5	638.5	235821.9	0.649	5.0	2325.6	0.728	0.649	0.728
0.46	4870.	34.4	2226.5	238048.4	0.655	15.7	2341.3	0.733	0.655	0.733
0.38	4120.	33.5	1569.6	239618.0	0.659	12.8	2354.1	0.737	0.659	0.737
0.94	5090.	33.9	4809.2	244427.2	0.673	32.0	2386.1	0.747	0.673	0.747
0.29	4920.	34.2	1424.6	245851.8	0.676	9.9	2396.0	0.750	0.677	0.750
0.20	4350.	33.6	861.8	246713.6	0.679	6.7	2402.7	0.752	0.679	0.752
0.14	8030.	32.7	1101.3	247814.9	0.682	4.5	2407.2	0.754	0.682	0.754
0.38	4100.	34.8	1562.0	249377.0	0.686	13.2	2420.4	0.758	0.686	0.758
0.49	4390.	35.5	2140.8	251517.8	0.692	17.3	2437.7	0.763	0.692	0.763
1.65	5160.	32.5	8492.5	260010.3	0.715	53.5	2491.2	0.780	0.715	0.780
0.27	4010.	31.2	1100.0	261110.3	0.718	8.6	2499.7	0.783	0.719	0.783
0.03	5010.	30.2	152.7	261263.0	0.719	0.9	2500.6	0.783	0.719	0.783
0.44	7360.	31.9	3252.7	264515.6	0.728	14.1	2514.8	0.788	0.728	0.788
0.15	7060.	34.2	1075.9	265591.5	0.731	5.2	2520.0	0.789	0.731	0.789
0.38	6650.	32.6	2533.5	268125.1	0.738	12.4	2532.4	0.793	0.738	0.793
0.30	1530.	32.9	466.3	268591.4	0.739	10.0	2542.4	0.796	0.739	0.796
0.24	1540.	29.4	375.5	268966.9	0.740	7.2	2549.6	0.798	0.740	0.798
0.21	1200.	29.4	256.0	269222.9	0.741	6.3	2555.9	0.800	0.741	0.800
0.08	3230.	35.1	246.1	269469.0	0.741	2.7	2558.5	0.801	0.742	0.801
0.24	1200.	30.2	292.6	269761.6	0.742	7.4	2565.9	0.804	0.742	0.804
0.17	1200.	33.7	201.2	269962.8	0.743	5.7	2571.6	0.805	0.743	0.805
0.27	2500.	35.6	685.8	270648.5	0.745	9.8	2581.3	0.808	0.745	0.808
0.20	1040.	36.0	206.0	270854.6	0.745	7.1	2588.4	0.811	0.745	0.811
0.24	2500.	33.4	609.6	271464.1	0.747	8.1	2596.6	0.813	0.747	0.813
0.37	3000.	33.9	1097.2	272561.4	0.750	12.4	2609.0	0.817	0.750	0.817
0.41	5270.	33.8	2168.4	274729.7	0.756	13.9	2622.9	0.821	0.756	0.821
0.52	6440.	32.1	3336.8	278066.5	0.765	16.6	2639.5	0.827	0.765	0.827
0.43	5280.	32.3	2253.0	280319.5	0.771	13.8	2653.3	0.831	0.771	0.831
0.21	6910.	32.9	1474.2	281793.8	0.775	7.0	2660.3	0.833	0.775	0.833
0.26	5260.	31.7	1362.7	283156.4	0.779	8.2	2668.5	0.836	0.779	0.836
0.34	6100.	32.0	2045.1	285201.6	0.785	10.7	2679.3	0.839	0.785	0.839
0.24	4860.	32.5	1185.0	286386.6	0.788	7.9	2687.2	0.842	0.788	0.842
0.24	4500.	32.5	1097.2	287483.8	0.791	7.9	2695.1	0.844	0.791	0.844
0.38	6810.	33.8	2594.5	290078.3	0.798	12.9	2708.0	0.848	0.798	0.848
0.27	1520.	34.3	416.9	290495.2	0.799	9.4	2717.4	0.851	0.799	0.851
0.12	5760.	32.3	702.2	291197.4	0.801	3.9	2721.3	0.852	0.801	0.852
0.14	5240.	33.1	718.7	291916.1	0.803	4.5	2725.9	0.854	0.803	0.854
0.11	4780.	33.2	509.9	292426.0	0.805	3.5	2729.4	0.855	0.805	0.855
0.27	4840.	32.9	1327.6	293753.7	0.808	9.0	2738.5	0.858	0.808	0.858
0.43	5200.	32.5	2218.8	295972.5	0.814	13.9	2752.3	0.862	0.814	0.862
0.34	4640.	32.8	1555.6	297528.1	0.819	11.0	2763.3	0.865	0.819	0.865
0.23	4420.	31.9	1010.4	298538.5	0.821	7.3	2770.6	0.868	0.822	0.868
0.18	5520.	31.1	1009.4	299547.9	0.824	5.7	2776.3	0.869	0.824	0.869
0.21	2740.	32.7	584.6	300132.5	0.826	7.0	2783.3	0.872	0.826	0.872

0.30	5100.	31.0	1554.4	301686.9	0.830	9.4	2792.7	0.875	0.830	0.875
0.47	3350.	31.4	1582.6	303269.5	0.834	14.8	2807.5	0.879	0.835	0.879
0.34	6890.	31.7	2310.0	305579.5	0.841	10.6	2818.2	0.883	0.841	0.883
0.62	5150.	32.7	3217.8	308797.3	0.850	20.4	2838.6	0.889	0.850	0.889
0.30	5610.	31.7	1709.8	310507.1	0.854	9.7	2848.2	0.892	0.854	0.892
0.17	4630.	31.2	776.1	311283.2	0.9	5.2	2853.5	0.894	0.857	0.894
0.44	6090.	32.1	2691.4	313974.6	0.9	14.2	2867.6	0.898	0.864	0.898
0.34	4590.	31.8	1538.9	315513.5	0.9	10.7	2878.3	0.901	0.868	0.901
0.56	5150.	31.0	2903.8	318417.3	0.9	17.5	2895.8	0.907	0.876	0.907
0.55	6470.	31.4	3549.5	321966.9	0.9	17.2	2913.0	0.912	0.886	0.912
0.30	6010.	32.2	1831.8	323798.6	0.9	9.8	2922.8	0.915	0.891	0.915
0.30	6530.	32.0	1990.2	325788.9	0.9	9.7	2932.5	0.918	0.896	0.918
0.46	5140.	31.1	2349.9	328138.8	0.9	14.2	2946.8	0.923	0.903	0.923
0.34	5240.	31.8	1756.8	329895.6	0.9	10.6	2957.4	0.926	0.908	0.926
0.08	4900.	31.0	373.4	330268.9	0.9	2.4	2959.8	0.927	0.909	0.927
0.24	5540.	30.7	1350.8	331619.7	0.9	7.5	2967.3	0.929	0.913	0.929
0.09	5450.	31.2	498.3	332118.0	0.9	2.9	2970.1	0.930	0.914	0.930
0.20	4390.	30.9	869.7	332987.7	0.9	6.1	2976.2	0.932	0.916	0.932
0.44	4160.	29.6	1838.5	334826.2	0.9	13.1	2989.3	0.936	0.921	0.936
0.03	3500.	30.7	106.7	334932.9	0.9	0.9	2990.2	0.936	0.922	0.936
0.44	4700.	29.2	2077.1	337010.0	0.9	12.9	3003.1	0.941	0.927	0.941
0.30	3910.	29.8	1191.7	338201.7	0.9	9.1	3012.2	0.943	0.931	0.943
0.26	3840.	30.4	994.8	339196.5	0.9	7.9	3020.1	0.946	0.933	0.946
0.34	3770.	30.1	1263.9	340460.5	0.9	10.1	3030.2	0.949	0.937	0.949
0.41	3330.	29.4	1370.2	341830.6	0.9	12.1	3042.3	0.953	0.941	0.953
0.06	2620.	28.5	159.7	341990.3	0.9	1.7	3044.0	0.953	0.941	0.953
0.06	3030.	27.8	184.7	342175.0	0.9	1.7	3045.7	0.954	0.942	0.954
0.59	2770.	30.1	1646.3	343821.3	0.9	17.9	3063.6	0.959	0.946	0.959
1.04	4020.	29.3	4165.8	347987.1	1.0	30.4	3094.0	0.969	0.958	0.969
0.35	5750.	29.5	2015.4	350002.5	1.0	10.3	3104.4	0.972	0.963	0.972
0.44	5970.	30.6	2638.4	352640.9	1.0	13.5	3117.9	0.976	0.970	0.976
0.44	3570.	31.5	1577.7	354218.6	1.0	13.9	3131.8	0.981	0.975	0.981
0.06	3940.	28.5	240.2	354458.8	1.0	1.7	3133.5	0.981	0.975	0.981
0.03	997.	28.9	30.4	354489.2	1.0	0.9	3134.4	0.982	0.975	0.982
0.43	969.	30.4	413.5	354902.7	1.0	13.0	3147.4	0.986	0.977	0.986
0.37	3310.	31.5	1210.6	356113.3	1.0	11.5	3158.9	0.989	0.980	0.989
0.52	4070.	30.6	2108.8	358222.1	1.0	15.8	3174.7	0.994	0.986	0.994
0.85	3860.	31.9	3294.1	361516.2	1.0	27.2	3202.0	1.003	0.995	1.003

SUM KH = 361516.18

SUM Φh = 3201.98

The cumulative flow capacity (CFC) and the cumulative storage capacity (CSC) were calculated and shown in (Table 3). Since the entire area was cored, it was possible to develop a flow unit zonation.

A cross plot of CFC and CSC was constructed for every well to reveal the vertical variation of flow capacity with unit storage (Figure 11). On this plot, flow units are differentiated by slope inflection. The inflection points are indicative of the three flow units (FU 1 to FU 3) present in the D-3 reservoir. Shaly interval are seen to plot as low-angle to horizontal trending flow units (FU 2), whereas the sandy interval exhibit a steeper gradient slope (FU 1 and FU 3) on the SML plot.

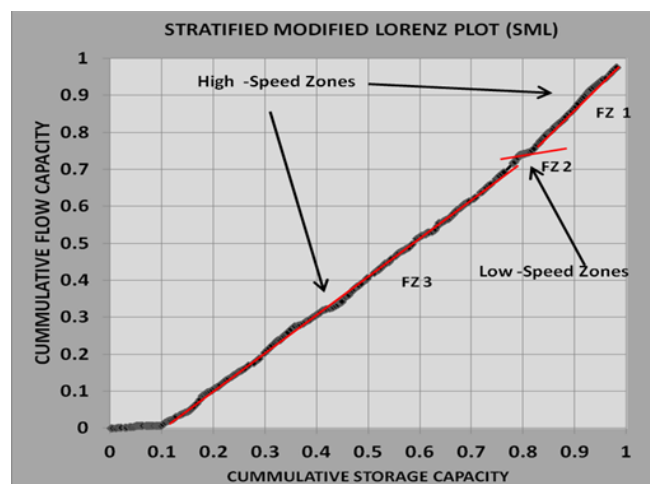


Fig 11 SML Plot of the Cumulative Storage Capacity Versus Cumulative flow Capacity for A2P2 Core Data Showing 3 flow Units

(Slatt, 2006) showed that similar technique was used in a research well drilled in Wyoming of which 10 flow units were identified from the research. From the study on Vin field, it is clear that the flow unit that contributes the most to the overall cumulative storage capacity and cumulative flow

capacity are the sandy intervals. According to (Rushing and Newsham, 2001) the slope determines whether the flow unit is a reservoir, baffle or seal (Fig 12). Conclusively, the D-3 reservoir Vin field is fairly homogenous and there is no shale baffle or seals.

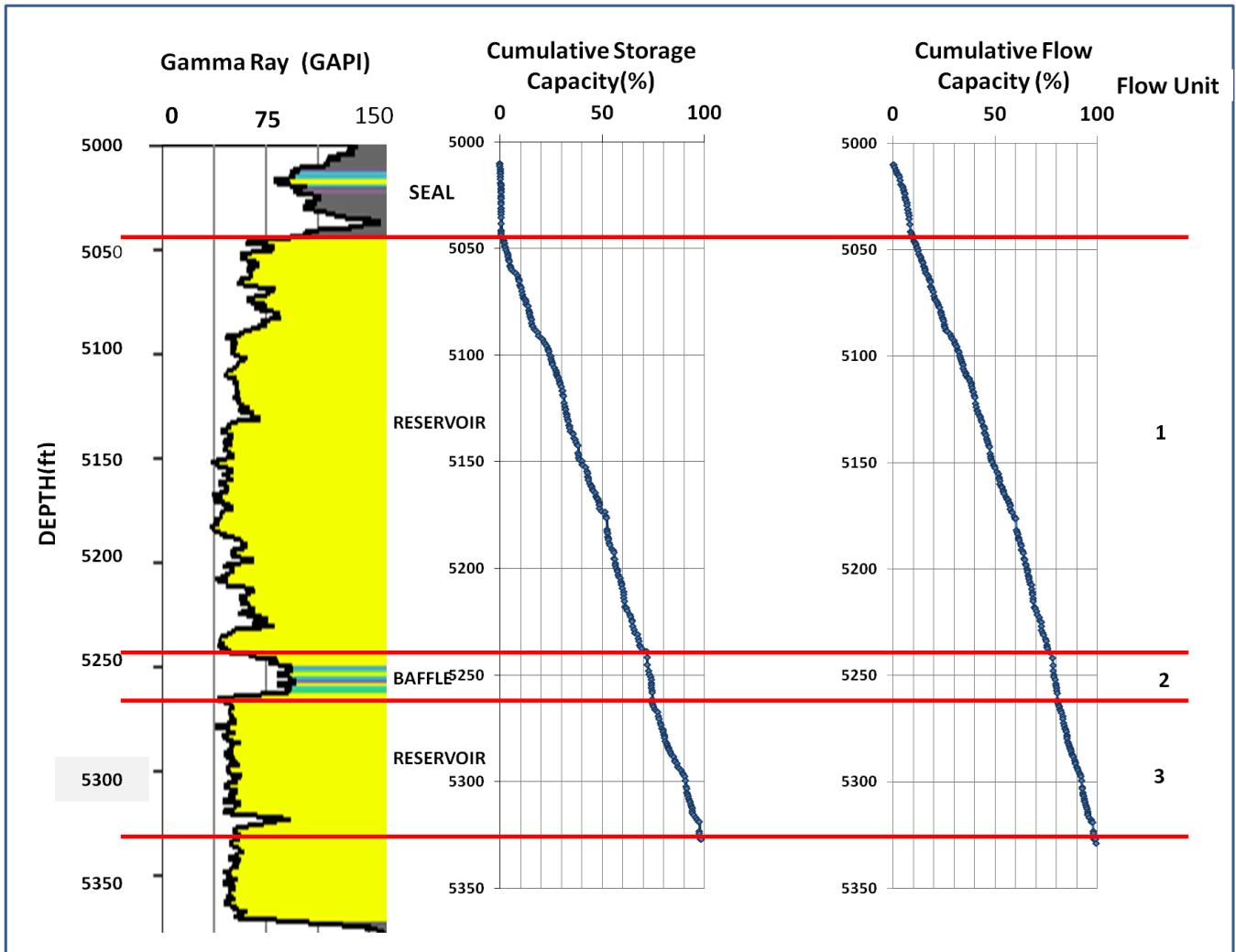


Fig 12 Depth Plot of Gamma-ray Log, Cumulative Storage Capacity, and Cumulative flow Capacity for D4 Reservoir Showing 3 flow Units

➤ *Flow Zone Indicator Plot (Fzi)*

Amaefule et al., (1993) and Tiab, (2000) developed a technique for identifying and characterizing a formation having similar hydraulic characteristics, or flow units based on the microscopic measurements of rock core samples. Flow zone indicator (FZI) plot was used to identify the various rock units in the reservoir complex. Flow zone indicator (FZI) is the slope of log –log plot between Rock quality index (RQI) and porosity (Phi-Z).

$$FZI = RQI / \Phi\text{-}Z$$

$$RQI = 0.0314 * \text{sqrt.} (\text{Perm}(K)/\text{Porosity}(\Phi))$$

$$\Phi\text{-}Z = \Phi / (100 - \Phi) \quad (\text{Adopted from Djebba and Donaldson, 2004})$$

Where:

FZI= Flow Zone Indicator
RQI= Reservoir Quality Index

Phi-Z= Normalized Porosity Index (Ratio of Pore volume to grain volume)

Since permeability and porosity can be measured from core samples, Phi-Z , RQI, FZI can be gotten according to above equations .

Flow zone indicator depends on geological characteristics of the material and various pore geometry of a rock mass; hence, it is a good parameter for determining hydraulic flow units (HFU) (Adnan)2014.

In this research, the flow unit concept was selected for subdivision of the reservoir into distinct petrophysical type. Each distinct reservoir type has a unique Flow Zone Indicator (FZI) value. Table 12 highlights the RQI, Phi-Z, and the FZI of the cored sample of A2P2 well, Vin field.

Table 4 Showing the Reservoir Quality Index(RQI) and Normalized porosity (ϕZ) of the D5 reservoir

Depth(ft)	Porosity (ϕ)	Permeability k (md)	RQI	ϕZ	FZI
5200.60	32.1	4670	0.3786	0.4734	0.7997
5201.30	34.0	5150	0.3867	0.5141	0.7522
5203.00	32.0	4720	0.3814	0.4705	0.8106
5203.80	31.3	5220	0.4053	0.4561	0.8887
5204.60	31.1	4700	0.3858	0.4521	0.8533
5206.00	30.1	2010	0.2566	0.4306	0.5959
5207.00	30.6	4340	0.3738	0.4416	0.8464
5207.60	31.9	5410	0.4086	0.4693	0.8707
5209.35	32.7	7680	0.4811	0.4862	0.9895
5211.00	33.9	3540	0.3207	0.5139	0.6240
5212.00	33.5	3020	0.2981	0.5038	0.5918
5213.70	34.6	3030	0.2937	0.5296	0.5547
5215.20	34.8	2900	0.2866	0.5337	0.5370
5217.90	35.2	6530	0.4277	0.5432	0.7874
5218.10	34.2	3020	0.2951	0.5198	0.5677
5218.60	34.0	4410	0.3575	0.5157	0.6932
5219.80	34.2	4520	0.3609	0.5199	0.6942
5221.60	35.1	4100	0.3394	0.5408	0.6275
5222.70	33.5	6280	0.4300	0.5034	0.8542
5224.20	32.9	3000	0.2998	0.4903	0.6115
5224.80	32.5	4190	0.3564	0.4820	0.7394
5226.95	34.4	4870	0.3734	0.5254	0.7106
5228.60	33.5	4120	0.3482	0.5038	0.6912
5230.10	33.9	5090	0.3849	0.5122	0.7516
5230.90	34.2	4920	0.3768	0.5191	0.7257
5232.90	33.6	4350	0.3570	0.5071	0.7041
5234.00	32.7	8030	0.4922	0.4856	1.0136
5235.80	34.8	4100	0.3410	0.5327	0.6402
5236.65	35.5	4390	0.3491	0.5508	0.6339
5237.45	32.5	5160	0.3958	0.4810	0.8228
5238.95	31.2	4010	0.3560	0.4534	0.7851
5241.80	30.2	5010	0.4046	0.4321	0.9365
5245.20	31.9	7360	0.4767	0.4691	1.0163
5247.90	34.2	7060	0.4510	0.5204	0.8665
5249.65	32.6	6650	0.4483	0.4844	0.9255
5250.70	32.9	1530	0.2141	0.4903	0.4367
5252.10	29.4	1540	0.2273	0.4160	0.5466
5253.80	29.4	1200	0.2006	0.4164	0.4817
5254.70	35.1	3230	0.3012	0.5410	0.5567
5255.80	30.2	1200	0.1979	0.4327	0.4575
5257.20	33.7	1200	0.1873	0.5091	0.3679
5258.30	35.6	2500	0.2632	0.5521	0.4768
5261.40	36.0	1040	0.1689	0.5615	0.3007
5262.95	33.4	2500	0.2717	0.5015	0.5417
5263.90	33.9	3000	0.2954	0.5129	0.5760
5264.70	33.8	5270	0.3922	0.5101	0.7688
5266.05	32.1	6440	0.4449	0.4721	0.9424
5266.60	32.3	5280	0.4012	0.4780	0.8393
5267.50	32.9	6910	0.4551	0.4901	0.9287
5269.10	31.7	5260	0.4045	0.4640	0.8719
5270.45	32.0	6100	0.4333	0.4713	0.9195
5272.35	32.5	4860	0.3838	0.4822	0.7959
5273.50	32.5	4500	0.3695	0.4815	0.7674
5274.90	33.8	6810	0.4460	0.5096	0.8753
5275.45	34.3	1520	0.2090	0.5226	0.3999
5276.55	32.3	5760	0.4190	0.4781	0.8765
5277.90	33.1	5240	0.3948	0.4959	0.7961

5278.60	33.2	4780	0.3768	0.4970	0.7581
5279.50	32.9	4840	0.3806	0.4911	0.7750
5281.10	32.5	5200	0.3972	0.4813	0.8252
5281.90	32.8	4640	0.3737	0.4871	0.7672
5282.80	31.9	4420	0.3695	0.4690	0.7877
5283.80	31.1	5520	0.4181	0.4521	0.9248
5284.30	32.7	2740	0.2873	0.4863	0.5909
5284.80	31.0	5100	0.4029	0.4488	0.8976
5285.70	31.4	3350	0.3245	0.4569	0.7104
5286.85	31.7	6890	0.4631	0.4635	0.9993
5287.65	32.7	5150	0.3941	0.4858	0.8111
5288.30	31.7	5610	0.4178	0.4637	0.9010
5289.80	31.2	4630	0.3826	0.4532	0.8443
5290.60	32.1	6090	0.4328	0.4718	0.9174
5291.40	31.8	4590	0.3774	0.4659	0.8100
5293.00	31.0	5150	0.4050	0.4484	0.9033
5293.65	31.4	6470	0.4505	0.4585	0.9825
5294.50	32.2	6010	0.4291	0.4744	0.9046
5295.90	32.0	6530	0.4488	0.4697	0.9557
5296.60	31.1	5140	0.4036	0.4516	0.8937
5297.50	31.8	5240	0.4034	0.4652	0.8670
5299.30	31.0	4900	0.3949	0.4489	0.8797
5302.40	30.7	5540	0.4215	0.4438	0.9498
5303.20	31.2	5450	0.4150	0.4535	0.9150
5305.00	30.9	4390	0.3744	0.4468	0.8380
5305.90	29.6	4160	0.3725	0.4196	0.8878
5306.65	30.7	3500	0.3351	0.4437	0.7552
5307.90	29.2	4700	0.3987	0.4114	0.9690
5308.80	29.8	3910	0.3596	0.4247	0.8469
5309.60	30.4	3840	0.3529	0.4366	0.8083
5310.80	30.1	3770	0.3513	0.4310	0.8152
5311.70	29.4	3330	0.3339	0.4173	0.8001
5312.55	28.5	2620	0.3011	0.3985	0.7556
5313.80	27.8	3030	0.3276	0.3857	0.8495
5314.75	30.1	2770	0.3010	0.4316	0.6974
5315.60	29.3	4020	0.3676	0.4149	0.8861
5316.90	29.5	5750	0.4387	0.4175	1.0509
5317.80	30.6	5970	0.4385	0.4411	0.9941
5318.85	31.5	3570	0.3345	0.4590	0.7287
5318.90	28.5	3940	0.3694	0.3979	0.9284
5323.10	28.9	997	0.1845	0.4062	0.4542
5324.20	30.4	969	0.1773	0.4369	0.4058
5326.25	31.5	3310	0.3219	0.4596	0.7006
5326.90	30.6	4070	0.3623	0.4403	0.8228
5327.10	31.9	3860	0.3453	0.4690	0.7361

A log-log plot of RQI versus ϕz was plotted for the samples, and all the samples with similar FZI values belong to the same hydraulic unit and will, therefore, lie on the same straight line (Amaefula et al., 1996), while samples

with different FZI will lie on other parallel lines (Figure 13). This shows that there are 3 flow units (FZ-1 to FZ-3) in the reservoir. In addition, the clustering of the FZI also depicts 3 flow units in the reservoir.

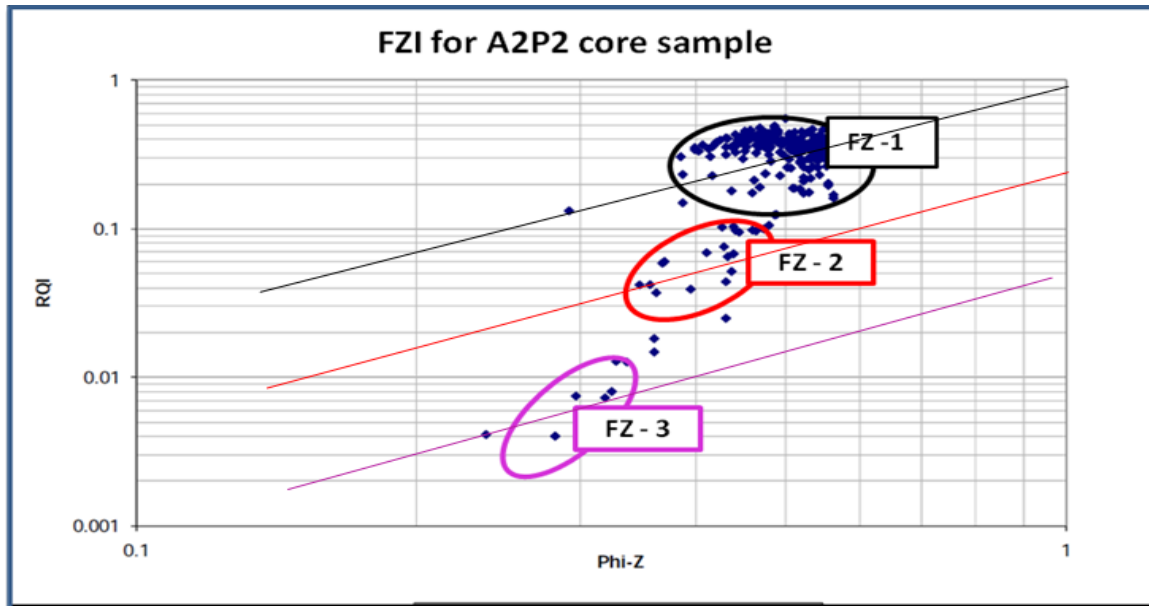


Fig 13 FZI Plot for A2P2 Core Data Vin Field Confirming the Presence of 3 flow Units

➤ Porosity-Permeability Cross Plot

Furthermore, porosity-permeability crossplot derived from well log data was used to identify the flow zones in the Vin field. From the result (Fig 14), samples on the same cluster have similar pore-throat feature and belong to one flow zone. Rocks containing authogenic pore lining, pore filling and pore bridging as well as fine grained poorly sorted sand tend to exhibit high surface area and high tortuosity hence low FZI. In contrast, less shaley, coarse-grained, and well sorted sand exhibit a lower surface area, lower tortuosity and higher FZI. Figure 14 showed that three distinct facies were analysed based on ditch cuttings description. These facies are: U1- fine grained well sorted sandstone, U2- very fine grained well sorted sandstone, and U3- very fine grained shaley sandstone. Each of these facies is associated to a unique flow unit. This means that different depositional environment and diagenetic processes control the geometry of the reservoir and consequently the flow unit index. But the trend observed reveals sediment deposited under the same condition (same depositional process and under the same depositional conditions) because majority of the flow unit occur in FZ-1 and U1.

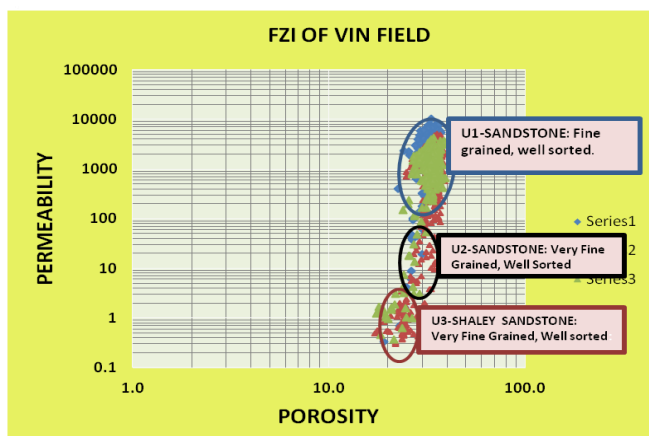


Fig 14 Flow Zone Indicator Plot for well A2, A19, and A20 Vin Field Confirming the Presence of 3 Flow Unit

➤ Winland Plot

Winland technique is based on characterisation of flow unit conditioned to the pore throat size of the rock unit. In this approach, a mathematical relationship is created between the petrophysical properties such as porosity, permeability and capillary pressure to the pore-throat radius measured in a mercury injection capillary pressure at mercury saturation of 35% (Gunter et al., 1997). The Winland equation is:

$$\log R35 = 0.732 + 0.588 \log K_{air} - 0.864 \log \phi_{core}$$

Where R35 is the pore throat radius corresponding to the 35th percentile of mercury saturation in a mercury capillary pressure test, K_{air} is the uncorrected air permeability (in mD), and ϕ is porosity (in %). The R35 method was used in this study as a tool to assign flow units.

Winland correlated porosity and permeability to pore throat radii corresponding to different mercury saturations. Using the standard classification for the pore throat size of the rock, R35 (Pore throat size) is generally classified into: 0.1, 0.5, 2, 5, 20 and 30 microns (Figure 15). The porosity and permeability plot of the A2P2 core data will fall into any of the classes. The result clearly shows that the core sample with similar R35 values represent a single rock and most of the core sample data have high permeability since they correlate with the 20 and 30 microns of the R35 pore throat size. Figure 16 also showed different reservoir rock types (RT) for cores using the Winland R35 plot. The core samples of similar R35 values represent a single rock type. Three reservoir rock types were identified, where RT3, has the highest permeability (higher than 1000 mD), and RT2, having moderate permeability (between 20 and 100 mD), are reservoirs. RT1 is not a reservoir rocks, because have very low permeability's, less than 20 mD. A summary of petrophysical characteristics for each UF is shown in Table 5, where FZI is the flow zone, ϕ (%) and K (mD) were determined in laboratory, and R35 is the Winland measure. In this Table 5, we can see that there are many

concordances between the different results, especially among the PF, the FZI and RT.

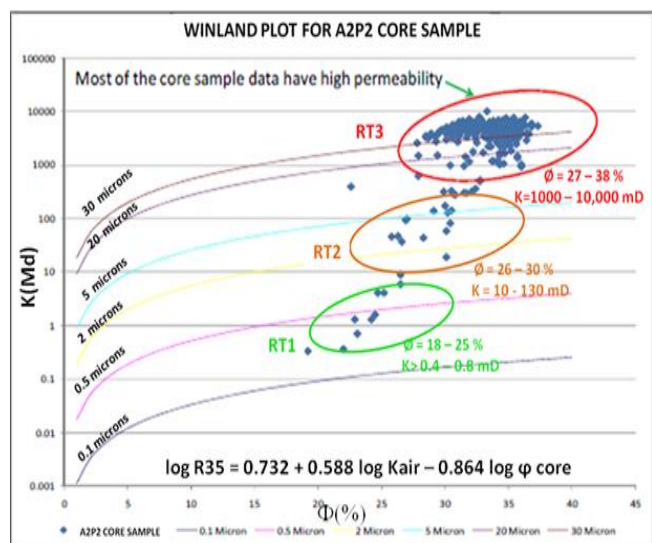


Fig 15 Winland Plot for A2P2 Core Sample D3 Reservoir Vin Field

- Showing Different RT

Units of flow	Petrophysical Characteristics				
	φ %	K (mD)	R35	R35 CLASS	RT
FZ-1	32	>1000	20-30	Megaport	RT 3
FZ-2	27	>10-130	2-5	Macroport	RT 2
FZ-3	22	>0.5-0.8	0.1-0.5	Microport	RT 1

Fig 16 Petro physical Characteristics of the Various flow Units in the D-3 Reservoir Sand Vin Field

V. SUMMARY AND CONCLUSION

The integration of data from core analysis, production data, seismic data, and petrophysical parameters, was very useful in the petrophysical reservoir characterization and assessment of the flow zones in the Vin field. Results showed that the reservoir is laterally extensive and thins gradually towards the west. Reservoir rock qualities were generally very good to excellent. Based on the FZI, three flow units (FZ-1 to FZ-3) were identified in the reservoir with FZ-1 having the best reservoir quality. The Stratified Modified Lorenz (SML) plot revealed three flow units with two high speed zones (FZ 1 and FZ 3) and one low speed zone (FZ 2). Based on the SML slope, the D-3 reservoir is fairly homogenous and there are no shale baffle or seals.

Winland technique revealed three Petrofacies (Mega porous, Macro porous, Micro porous), with different rock types. Porosity-permeability cross plot also revealed three distinct facies based on ditch cuttings description. These facies are: U1- fine grained well sorted sandstone, U2- very fine grained well sorted sandstone, and U3- very fine grained shaley sandstone. Each of these facies is associated to a unique flow unit meaning that different depositional environment and diagenetic processes control the geometry of the reservoir and consequently the flow unit index. A summary of petrophysical characteristics for each flow zone showed that there are many concordances between the different results, especially among the PF, the FZI and RT. Using the proposed integrated methodology has lead to a significantly more accurate petrophysical reservoir description and 3-D reservoir model, which can be used to forecast reservoir behavior and enhance recovery.

ACKNOWLEDGEMENT

The management of Moni Pulo Limited, Port Harcourt, and the O.B Lulu Briggs Chair in Petroleum Geosciences, Institute of Petroleum Studies, University of Port Harcourt, Nigeria, is well appreciated for providing the available data used to carry out this study. I acknowledge with thanks the technical contributions of Mr Kenneth Uhoo, and Mr Bamibgoye Ebenezer.

REFERENCES

- [1]. Adaeze, I.U., Samuel, O. O. and Chukwuma, J.I. (2012). Petrophysical Evaluation of Uzek Well Using Well Log and Core Data, Offshore Depobelt, Niger Delta, Nigeria. *Advances in Applied Science Research*, 3(5), 296-299.
- [2]. Adeel, N.R., Shabeer, A. A and Sarfraz, H. S. (2016). Sedimentary Facies Interpretation of Gamma Ray(GR) Log as Basic Well Logs in Central and Lower Indus Basin of Pakistan. *Geodesy and Geodynamics*. 7(6), 432 – 443.
- [3]. Adnan, A. A. (2014). Hydraulic Flow Units and Permeability Prediction in a Carbonate Reservoir, Southern Iraq from Well Log Data Using Non Parametric Correlation, *International Journal of Enhanced Research in Science Technology and Engineering*, 3(1), 480-486.
- [4]. Ahmed, K. J. and Muhannad, T. S. (2012) Multiple Linear Regression Approach for the Permeability Calculation from Well Logs: A Case Study in Nahr Umr Formation - Subba Oil Field, Iraq, *International Journal of Science and Research (IJSR)*, P.1- 8.
- [5]. Alejandro, E. (2006). Petrophysical and seismic properties of lower Eocene clastic rocks in the central Maracaibo Basin. *A.A.P.G Bull. Vol.90*, P. 679-696.
- [6]. Amaefule, J. O., Altunbay, M.H., Tiab, D., Kersey, D. G. and Keelan, D. K. (1993). Enhanced Reservoir Description: Using Core and Log Data to Identify Hydraulic (Flow) Units and Predict Permeability in Uncored Intervals/Wells. SPE Annual Technical Conference and Exhibition. Society of Petroleum Engineers, P. 205 – 220.

- [7]. Asquith, G. and Krygowski, D. (2004). Basic Well Log Analysis. AAPG Methods in Exploration Series, Manchester, United Kingdom. Vol. 2, P. 23-59.
- [8]. Asquith, G.B. and Gibson, C.R. (1982). Basic Well Log Analysis for Geologists. 3rd Printing, Published by A. A. P.G, Tulsa Oklahoma USA. 216p.
- [9]. Bhattacharya, S., Alan, P. B., Watney, W. L. and Doveton, J.H. (2008). Flow unit modelling and fine-scale predicted permeability validation in Atokan sandstones: Norcan East field, Kansas, A.A.P.G Bull, Vol. 92, No. 6, P. 709–732.
- [10]. Chow, J. J., Ming, C. L. and Fuh, S. (2005). Geophysical well logs study on the paleoenvironment of the hydrocarbon producing zones in the Erchungchi Formation, Hsinyin, SW Taiwan. Vol.16, No.3, P. 531-54
- [11]. Corredor, F., Shaw, J.H. and Bilohi. (2005). Structural Styles in the deepwater fold and thrust belts of the Niger Delta. A.A.P.G Bull, Vol.89, No. 6, P.753-780.
- [12]. Doust, H., and Omatsola, E., 1990. Niger Delta, in Edwards, J.D., and Santogrossi, P.A., eds., Divergent/Passive Margin Basins, AAPG Memoir 48: Tulsa, American Association of Petroleum Geologists, pp 239-248.
- [13]. Dubois, M. K., Byrnes, A.P., Bohling, G.C. and Doveton, J.H. (2006). Multiscale geologic and petrophysical modelling of the giant Hugoton gas field (Permian), Kansas and Oklahoma, U.S.A., in P. M. Harris and L. J. Weber, eds., Giant hydrocarbon reservoirs of the world: From rocks to reservoir characterization and modelling. A.A.P.G Memoir 88/SEPM Special Publication, P.307– 353.
- [14]. Ebanks, W. J. (1987). The Flow Unit Concept-An Integrated Approach to Reservoir Description for Engineering Projects. Am. Assoc. Geol. Annual Convention, P. 1022 – 1145.
- [15]. Ebanks, W. J., Scheihing, M.H. and Atkinson, C.D., (1992). Flow units for reservoir characterization. In: Thompson, D.M. and A. M .Woods, (eds.), Development Geology Reference Manual, Amer. Assoc. Petrol. Geol. Methods in Exploration Series No. 10, P. 282–285.
- [16]. Edigbue, P. I., Komolafe, A.A., Adesida, A.A. and Itamuko, O.J. (2014). Hydrocarbon reservoir characterization of “Keke” field, Niger Delta using seismic and petrophysical data. American Journal of Scientific and Industrial Research, Vol. 5, Issue 2, P. 73-80.
- [17]. Ejedawe, J.E. (1981). Patterns of incidence of oil reserves in Niger Delta Basin. A. A. P. G Bull, Vol. 65, P. 1571 – 1585.
- [18]. Ekweozor, C.M. and Daukoru, E.M. (1984). Petroleum source bed evaluation of Tertiary Niger Delta. A. A .P G. Bull. Vol.68, P. 390 – 394.
- [19]. Emery, D. and Myers, K.J. (1996). Sequence Stratigraphy. Blackwell Science Ltd, 885.p
- [20]. Etu-Efeotor, J.O. (1997). Fundamentals of Petroleum Geology. Published by Paragraphics (an imprint of Jeson services), Port Harcourt. P.62, 64, 146.
- [21]. Evamy, B.D., Haremboure, J., Kamerling, P., Knaap, W.A., Molloy, F.A., and Rowlands, P.H., 1978, Hydrocarbon habitat of Tertiary Niger Delta: American Association of Petroleum Geologists Bulletin, v. 62, pp 277-298.
- [22]. Fadila, B. (2004). Reservoir Characterization and Reservoir modelling in the north-western part of Hassi Messaoud field Algeria. PhD Thesis Unpublished. 98 p.
- [23]. Gluyas, J.G. and Witton, T. (1997). Poroperm prediction for wildcat exploration prospects: Miocene Epoch, Southern Red Sea, in J.A. Kupecz, J. Gluyas, and S. Bloch, eds., Reservoir quality prediction in sandstones and carbonates: AAPG Memoir 69, P. 163–176.
- [24]. Harris, P. M. and Weber, L.J. (2006). Giant hydrocarbon reservoirs of the world: From rocks to reservoir characterization and modelling, In P. M. Harris and L. J. Weber. eds., Giant hydrocarbon reservoirs of the world: From rocks to reservoir characterization and modelling: A.A.P.G Memoir 88/SEPM Special Publication, P.1- 6.
- [25]. John, O. A. and Oluwaseyi, I. (2013). Petrophysical Properties Evaluation for Reservoir Characterisation of SEYI Oil Field (Niger-Delta). International Journal of Innovation and Applied Studies, Vol. 3, No. 3, P. 765-773.
- [26]. **Johnson, E. F., Bossler, D. P., Naumann, V. O., (1959)** "Calculations of Relative Permeability from Displacement Experiments." Technical Note 2027 JPT, Vol.198, pp. 61 – 63
- [27]. Jon, G. and Richard, S. (2004). Petroleum Geosciences. Blackwell Publishing, USA. P. 54 – 112.
- [28]. Joseph, M.B., Steven. L.G and Ronald, L.W., (2004):Gulf of Guinea Geology, Oil and Gas Journal, Pennywell 8pp
- [29]. Knox, G.J., and Omatsola, M.E., 1989, Development of the Cenozoic Niger Delta in terms of the escalator regression model, in Coastal Lowlands, Geology and geotechnology. Proc. Kon. Nederl. Geol. Mijnb. Genoots, pp 181-202.
- [30]. Lyon, W.C. (2010). Working Guide to Reservoir Engineering, Elsevier Burlington, USA, 316 p.
- [31]. Macdonald, A.C. and Aesan, J. O. (1995). A prototype procedure for stochastic modelling of facies tract distribution in shoreline reservoir. In J.M.Yarus and R.L Chambers, eds., Stochastic Modelling and Geostatistic: Principles, Methods and Case Studies, A.A.P.G Computer. P. 91 – 108.
- [32]. Makinde, F. A., Adefidipe, O. A. and Craig, A. J. (2011). Water Coning in Horizontal Wells: Prediction of Post-Breakthrough Performance. International Journal of Engineering and Technology. Vol. 11, No.1, P. 173-185.
- [33]. Mode, A.W. and Anyiam, A.O. (2007). Reservoir Characterization: Implications from Petrophysical Data of the Paradise-Field, Niger Delta, Nigeria. Pacific Journal of Science and Technology. Vol. 8, No 2, P. 194-202.

- [34]. Mohaghegh, S., Arefi, R., Ameri, S. and Hefner, M. H. (1994). A Methodological Approach for Reservoir Heterogeneity Characterization Using Artificial Neural Networks, SPE Annual Technical Conference and Exhibition, 4p
- [35]. Morad, S., Khalid, A., Ketzer, J.M. and De Ros, L.F. (2010). The impact of diagenesis on the heterogeneity of sandstone reservoirs: A review of the role of depositional facies and sequence stratigraphy, *A.A.P.G Bull*, Vol. 94, No. 8, P. 1267–1309.
- [36]. Nooruddin, H. (2011). Field Application of a Modified Kozeny-Carmen Correlation to Characterize Hydraulic Flow Units, SPE Technical Symposium and Exhibition AlKhobar, Saudi Arabia, P. 2-9.
- [37]. Odoh, B. I., Onyeji, J. and Utom, A. U. (2012). The Integrated Seismic Reservoir Characterization (ISRC), Study in Amboy Field of Niger Delta Oil Field – Nigeria, *Geosciences*, 2(3): p. 60-65
- [38]. Omoboriowo, A.O., Chiadikobi, K.C. and Chiaghanam, O.I. (2012). Depositional Environment and Petrophysical Characteristics of “LEPA” Reservoir, Amma Field, Eastern Niger Delta, Nigeria. *International Journal of Pure and Applied Sciences and Technology*, Vol. 10, No 2, P. 38 – 61
- [39]. Opafunso, F.O. (2007). 3D Formation evaluation of an oil field in the Niger Delta area of Nigeria using Schlumberger Petrel workflow tool. *Journal of Engineering and Applied Sciences*, Vol. 2, No.11, P.1651 – 1660.
- [40]. Orife, J. M. and Avbovbo, A. A. (1982): Stratigraphy and the unconformity traps in Niger Delta. *American Association of Petroleum Geologist Memoire*; Vol. 32, p. 265.
- [41]. Oyedele, K.F., Ogagarue, D.O. and Mohammed, D.U. (2013). Integration of 3D Seismic and Well log Data in the Optimal Reservoir Characterization of EMI Field, Offshore Niger Delta Oil Province, Nigeria. *American Journal of Scientific and Industrial Research*, Vol. 4, No.1, P.11 – 21.
- [42]. Reijers, T. J., Petters, S.W. and Nwajide, C.S. (1997). The Niger Delta. In: R.C. Selley (ed): *African Basins. Sedimentary Basin of the World 3*. Elsevier Amsterdam. P. 151-172.
- [43]. Reijers, T. J., (2011) .Stratigraphy and Sedimentology of the Niger Delta. *Geologos* 17(3): 133-162
- [44]. Reijers, T.J.A, 1996: Selected Chapters on Geology, "Sedimentary Geology, Sequence Stratigraphy, Three Case Studies, A Field Guide. SPDC reprographic Services Warri, Nigeria.
- [45]. Rider, M.H. (2002). *Well Geological Interpretation of Well Logs*: Interprint Ltd. Malt. 280 p.
- [46]. Saibal, B., Alan, P., Byrnes, R., Watney, W. and Doveton, J. (2008). Flow unit modelling and fine-scale predicted permeability validation in Atokan sandstones: Norcan East field, Kansas, *A.A.P.G Bull*, Vol. 92, No.6, P.709–732.
- [47]. Selley, R.C. (1998). *Elements of petroleum geology*. Department of Geology, Imperial College, London United Kingdom, P.37-145.
- [48]. Selley, R.C. (2000). *Applied Sedimentology*. Second edition. Royal school of mines, Imperial College London. Academic Press, P. 56 – 82
- [49]. Serra, O. (1985). *Sedimentary Environments from Wire line Logs*, Schlumberger, Houston, 211 p.
- [50]. Short, K.C., and Stauble, A.J., 1995. *Outline of Geology of Niger Delta: American Association of Petroleum Geologists Bulletin*, v. 51, pp. 761-779.
- [51]. Slatt, R.M. (2006). *Stratigraphic Reservoir Characterization for Petroleum Geologists, Geophysicists, and Engineers*. Elsevier publishing, Amsterdam, 478 p.
- [52]. Sneider, R.M. (1987). *Practical Petrophysics for Exploration and Development*. Amer. Assoc. Petrol. Geol. Short Course Lect. Notes, variously paginated.
- [53]. Spearing, M., Allen, T. and Gavin M. (2013). Review of the Winland R35 method for net pay definition and its application in low permeability sands in Kekeya Block, Tuha Basin, China. *The open Petroleum Engineering Journal*, Vol.8, P. 167 – 171.
- [54]. TareK, A. (2001). *Reservoir Engineering Handbook* Gulf Publishing Company, Houston, Texas, 1211p.
- [55]. Tiab, D. and Donaldson, E.C. (2004): *Petrophysics: Theory and Practice of Measuring Reservoir Rock and Fluid Transport Properties*. Elsevier Oxford, 926 p.
- [56]. Tinker, S.W. (1996). Building the 3-D jigsaw puzzle: Application of sequence stratigraphy to 3-D reservoir characterization, Permian Basin, *A. A.P.G. Bull*, Vol. 80, P. 460-482.
- [57]. Walid, M. M. (2005). BVW as an indicator for hydrocarbon and reservoir homogeneity, *Journal of Petroleum Science and Engineering*, Vol. 29, Issue 1-2, P. 57-64
- [58]. Wang, J., Liu, H., and Zenglin, W., 2012. Quantitative Models of Development Laws for Heterogeneous Sandstone Reservoirs by Water Flooding. *The Open Petroleum Engineering Journal*, Vol. 5, P. 26-35
- [59]. Weber, K.J., 1971. Sedimentological aspect of the oil fields in the Niger Delta: *Geologie en Mijnbouw*, vol .50, no .3, pages 559-576.
- [60]. Weber, K.J., and Daukoru, E.M., 1975, *Petroleum Geology of the Niger Delta: Proceedings of the Ninth World Petroleum Congress*, volume 2, Geology: London. Applied Science Publishers Ltd., pp 210-221.
- [61]. Wudiriri, B., Ezeh, F.P., Unomah, G., Gunter, M., Anene, C., Alofe, K. and Famurewa, O. (2013). An Integrated Reservoir Description for Geologic Modeling in Matured Fields. *N. A. P. E Bull*, Vol. 25, P. 224 – 245.